



Petrography and geochemistry of successions from northwest Bolivia

Udo Zimmermann^{a,*}, Shirley Lopez^b, Zohyab Afzal^a, Krishiat Alexandra Cuellar Guasde^{a,b}

^a Department of Energy Resources, University of Stavanger, Norway

^b Instituto de Investigaciones en Ingeniería Petrolera INSPET-Universidad Mayor de San Andrés, La Paz, Bolivia

ABSTRACT

A complete section of Paleozoic sedimentary rocks has been sampled in northwest Bolivia to investigate compositional changes based on petrographic but mainly geochemical data. Studies of Paleozoic succession in southern Peru, northern Chile and northwest Argentina allowed to decipher the paleotectonic history of the region for the Paleozoic (e.g. compilations in Bahlburg et al., 2009). However, a few is only known about the area geographically in between. We focus here on an area in the vicinity of the capital La Paz, where the Paleozoic belongs paleogeographically to the so-called 'altiplano' and the 'Cordillera Oriental del Norte' and tectonically to the 'Faja de Huarina del Norte'. The objective of the study is, hence, to establish a first complete stratigraphic insight of the Paleozoic to enable further studies on key formations or horizons. While the abovementioned areas to the north and south do reflect in the sedimentary record the emergence of a continental arc during the Ordovician, followed by a significant tectonic quiescence during the late Silurian and Devonian and succeeded by the evolution of a second active margin with a continental arc during the late Paleozoic, these events are not visible in the Bolivian samples which is sandwiched between the westerly Arequipa Massif and the eastern Sunsas belt, both composed of mainly metamorphic rocks.

The Paleozoic section in northwest Bolivia shows highly recycled quartz-arenites of Ordovician age followed by Silurian and Devonian successions mainly composed of subangular to surrounded detritus, moderately sorted, devoid of significant typical metamorphic detritus. During the late Paleozoic, the rocks tend to a larger variability, partly even poorly sorted, higher amount of angular grains and the occurrence of volcanoclastic debris. Geochemically the same trend can be observed, with strongly recycled successions during the Ordovician (Zr/Sc 20–200) followed by moderately recycled rocks (mainly Zr/Sc 10–20100) with typical trace element composition for unrecycled upper continental crust (UCC). During the Permian, sediments which are less weathered and slightly less fractionated in their overall geochemical composition, have been deposited. The geochemistry may point to the evolution of late Paleozoic volcanism, recorded in overlying, but however, Triassic rocks. Significant increase or even typical UCC values of compatible elements or ratios are absent besides Cr and Ni increase in Ordovician rocks. The absence of any significant input of arc related detritus can be explained by not effective sediment dispersal system to transport arc related detritus into the depositional area. The low compositional and low to moderate textural maturity throughout the entire post-Ordovician stratigraphy implies relatively proximal sources and insignificant intra-basinal recycling. This together with the absence of metamorphic detritus, allows in proposing thick homogeneous sedimentary successions with low or no metamorphic overprint as major sources. Those covered possibly the today exposed metamorphic successions of the aforementioned basin surroundings. Sedimentary or any other lithologies older than the Ordovician and younger than Mesoproterozoic are nearly unknown in the region, besides one exception (Chilla beds; Bahlburg et al., 2020). Those hypothetical deposits would be at this stage of knowledge the best explanation.

1. Introduction

In the central Andes in the area of northern Bolivia (region of La Paz; Fig. 1), a nearly complete Paleozoic stratigraphy is exposed, including two diamictite deposits, the Silurian Cancañiri Formation and the Devonian Cumaná Formation, both interpreted as glacial deposits (Díaz Martínez and Isaacson, 1994; Díaz Martínez and Grahn, 2007). However, a few is known about the successions within the regional geological framework. Compilation of mainly detailed and meticulous paleontological work had been published together with sedimentological studies mostly by regional authors (compiled in Suárez Sorucco and Díaz Martínez, 1996). Sketchy is the knowledge of the provenance of the clastic successions. While volcanic arcs have been established in the

Ordovician towards the north in Peru (Bahlburg et al., 2006, 2011) and to the south, in northwest Argentina (e.g. Pankhurst et al., 1998; Bahlburg, 1998; Zimmermann et al., 2003; Otamendi et al., 2020), nothing is known about a Lower Ordovician volcanic arc in Bolivia. Only one exemplary systematic study by Reimann Zumsprekel et al. (2015) addresses the here studied Ordovician successions and one Silurian formation of the region, but could not report significant remnants of a synsedimentary volcanic arc or detritus related to the Famatinian orogenic cycle (Bahlburg et al., 2009; Reimann et al., 2010; Reimann Zumsprekel et al., 2015). During the Carboniferous and Permian, subduction took place in northwest Argentina and Chile and is reflected in igneous and volcanoclastic rocks, (Breitkreuz et al., 1989; Breitkreuz and Zeil, 1994). Permo-Carboniferous subduction and volcanic activity in

* Corresponding author.

E-mail address: udo.zimmermann@uis.no (U. Zimmermann).

<https://doi.org/10.1016/j.jsames.2023.104280>

Received 15 November 2022; Received in revised form 9 February 2023; Accepted 23 February 2023

Available online 2 March 2023

0895-9811/© 2023 The Authors. Published by Elsevier Ltd. This is an open access article under the CC BY license (<http://creativecommons.org/licenses/by/4.0/>).

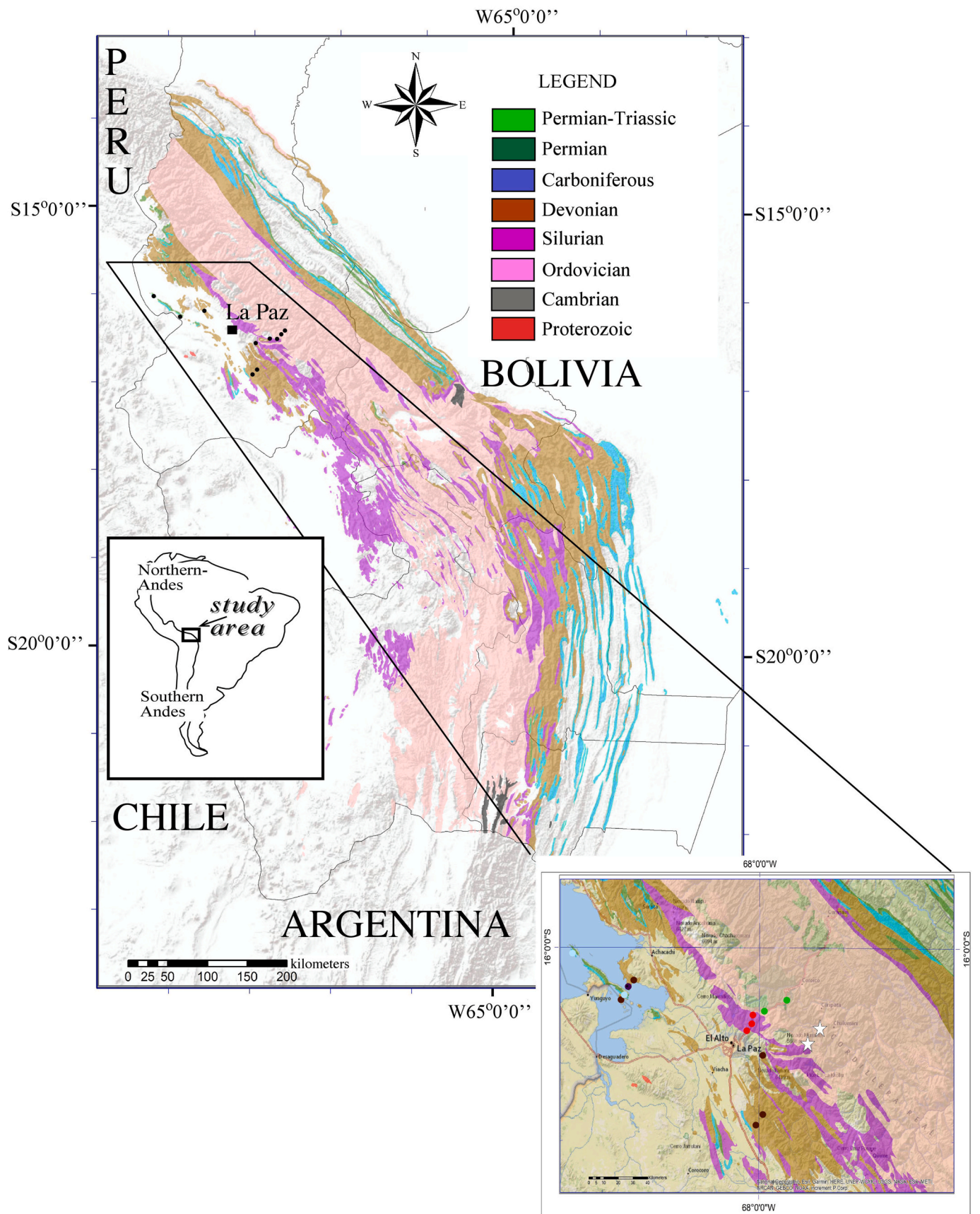


Fig. 1. Outcrop and geological map of La Paz region in the Central Andes (modified after SEGEOMIN-YFPB, 2001). Stars indicate the sample locations. GPS points in the text and in Supplementary Table 1.

Peru has been also identified (Díaz Martínez, 1995; Boekhout et al., 2018), but specific work on Upper Paleozoic Bolivian deposits in this regard is scarce.

The general geological evolution of the western margin of Gondwana, including Bolivia, based on largely detrital zircon studies using U–Pb and Lu–Hf from Paleozoic successions of the Central Andes has been presented by Bahlburg et al. (2009) and identified for the Paleozoic a magmatic arc related phase (Famatinian magmatic arc, 510 to 420 Ma), followed by a time of relative tectonic quiescence during the Devonian and the onset of magmatic activity during the Carboniferous until the end of the Paleozoic. However, studies on the entire Paleozoic stratigraphic package in terms of sediment geochemistry and petrography are absent.

Geochemical studies in northwestern Argentina and northern Chile on Lower Paleozoic rocks, have been able to identify changing paleotectonic settings and variation in the provenance of the detritus (e.g. Bahlburg, 1990, 1998; Bock et al., 2000; Zimmermann et al., 2003, 2010), but such a data set is, however, absent for Bolivia. This contribution here presents a first ‘standard’ of the geochemical composition throughout the Paleozoic of Bolivia and fills this void in our knowledge. This first overview will facilitate well-focussed future sampling for heavy mineral studies and detrital zircon geochronology to identify ages of sediment sources and may substantiate, or not, recycling of detritus during the Paleozoic.

1.1. Compiled geological evolution of northwest Bolivia and the regional framework

The here studied Paleozoic successions had been deposited in the so-called Peru-Bolivia Trough and add up to nearly 10 km of sedimentary rocks. The section begins during the Ordovician with sandstones and is followed by diamictite and again sandstones during the Silurian (Fig. 2). Devonian deposits are again mainly sandstones interrupted by diamictites which grade into red beds. During the Carboniferous carbonate deposits developed associated with sandstones and pyroclastic material. At the end of the Paleozoic interlayering of carbonates, marls, sandstone and pyroclastic rocks took place (Fig. 2). Overlying successions of Triassic age (Tiquina Formation, not here discussed) show then massive volcanism in form of mafic lava flows (Suárez Soruco and Díaz Martínez, 1996). Most of the successions have been deposited in shallow marine or platform environments despite the oldest – Ordovician – deposits and

possibly parts of the Lower Carboniferous Kasa Formation and the Upper Permian to Lower Triassic Chutani Formation (Suárez Soruco and Díaz Martínez, 1996).

The margin of western Gondwana was an area of nearly continuous subduction since at least the Cambrian (Ramos, 2000) or even earlier (Chew et al., 2007, 2008; Naidoo et al., 2016). The central Andes, a region here defined from southern Peru to northwest Argentina, experienced active subduction with the evolution of a magmatic arc during the Ordovician in northwest Argentina and southern Peru (compilations in Aceñolaza et al., 1996; Pankhurst et al., 1998; Bock et al., 2000; Zimmermann et al., 2003, 2010; Bahlburg et al., 2006, 2009; Reimann et al., 2010; Reimann Zumsprekel et al., 2015; Otamendi et al., 2020). The region of northwest to southwest Bolivia remains enigmatic in this regard. No record of subduction and arc magmatism can be stated from late Silurian to early Carboniferous for the same region (Fortey et al., 1992; Bahlburg and Herve', 1997; Chew et al., 2007; Cardona et al., 2009) with the development of a passive margin (Bahlburg and Herve', 1997; Cawood et al., 2012). Then, during the late Paleozoic subduction re-established expressed with the development of a volcanic arc (e.g. Breitzkreuz 1990; Boekhout et al., 2018), although not yet observed in Permo-Carboniferous deposits of northwestern Bolivian besides few volcanic ashes (e.g. Hamilton et al., 2016).

Reimann et al. (2010) define the Ordovician to Devonian deposits in northwestern Bolivia as part of the Peru-Bolivia Trough bounded to the west by the Arequipa Massif and to the east by the Amazonian craton. The Arequipa Massif is composed of gneisses and schists as well as high grade metamorphic rocks (Dalmayrac et al., 1977; Shackleton et al., 1979; Loewy et al., 2004). The eastern border is mainly represented by the Sunsas and Tucavaca belts and characterized by low but mainly medium grade to high grade metamorphic rocks (Litherland et al., 1986, 1989). Provenance studies for the study area in this contribution for the Amutara and Cancañiri formations point to a major provenance from the east, the Amazonian craton, using detrital zircon studies (Reimann et al., 2010). The same depositional center, the Peru-Bolivia trough, prolongs during the entire Paleozoic, sandwiched between the two mentioned orogens (França et al., 1995). The basin narrows significantly towards the south and in width during the Devonian and ended as a smaller entity during the Carboniferous and Permian (França et al., 1995). This constant existent depositional basin was, however, affected by tectonic movement as simple basin infill would have caused significant burial metamorphism within the lower Paleozoic successions (Mégard et al.,

Age	Formation	Major lithotypes
Guadalupian-Lower Triassic	CHUTANI	carbonates, volcanoclastics, marls, sandstones
Upper Carboniferous-Cisuralian	COPACABANA	carbonates, epiclastics, marls, sandstones
Upper Carboniferous	YAURICHAMBI	sandstones
Visean-Serpukhovian	SIRIPACA	silt- and sandstones with coal beds
Lower Carboniferous	KASA	sandstones, diamictite layers
Upper Devonian-Mississippian	CUMANA	silt- and sandstones, diamictite layers
Givetian-Frasnian	COLLPACUCHO	silt- fine sandstones with few shales
Lower to Middle Devonian	SICA SICA	silt- fine sandstones with few shales
Upper Pragian-Emsian	BELEN	silt- fine sandstones with shales
Lower Devonian	VILA VILA	silt- fine sandstones with few shales
Ludlow-Pridoli	CATAVI	silt- to sandstones
Wenlock-Ludlow	UNCIA	silt- to sandstone
Wenlock-Ludlow	CANCANIRI	silt- to sandstone, diamictite beds, shales
Katian-Sandbian	AMUTARA	quartz-arenites
Darriwillian	COROICO	quartz-arenites, shales

Fig. 2. Brief orientation of the stratigraphy and the here sampled units (after Suárez Soruco and Díaz Martínez, 1996).

1971; Cordani et al., 2019). Even conservative calculations of sedimentary thicknesses (see below) would result in 9–10 km of Paleozoic sediments. Reimann Zumsprekel et al. (2015) proposes a greenschist metamorphism based on the abundant chlorite within the Coroico Formation. We cannot state any metamorphic evidence higher than maximal very-low grade conditions within the successions, as new growth of mica or chlorite could not be observed and even the palynological record seems to be very well established and not affected by metamorphism (Zimmermann et al., 2015) in post-Ordovician successions. The fact of a constant sedimentary depositional center throughout the Paleozoic, also implies the opportunity of registering arc related detritus, produced during the Ordovician and the late Paleozoic. Unfortunately, nothing is known about major sediment transport directions in the study area.

1.2. Methodology and sampling

1.2.1. Optical petrography

From each formation studied (see below), 12–28 thin sections have been made and the most important characteristics are here presented.

1.2.2. Geochemistry

Major, trace and rare earth elements geochemistry analysis took place at Acme Laboratories (Canada). The method analysed machine-milled fine powders from 162 new rock samples for this study which are merged with 11 samples from the literature (Reimann Zumsprekel et al., 2015; see here for detailed sample preparation). The new rock material has been milled in agate mills after samples (devoid of veins) had been cleaned from alteration surfaces and analysed at Bureau Veritas Minerals laboratories in Canada. The samples were mixed with $\text{LiBO}_2/\text{Li}_2\text{B}_4\text{O}_7$ flux in crucibles and fused in a furnace. The resulted bead was cooled and dissolved in ACS grade nitric acid and analysed by Inductive Coupled Plasma-Mass Spectrometry (ICP-MS). Loss on ignition (LOI) was determined by igniting the sample with a known mass in a tarred crucible at 1000 °C for 1 h and calculating the difference in mass after the sample was cooled. Total Carbon and Sulfur were determined by the LECO® method. An additional 14 elements concentrated HCl, HNO_3 , and $\text{DI-H}_2\text{O}$ for 1 h in a heating block or hot water bath. The sample volume was increased with dilute HCl-solutions. Few samples have been analysed to decipher total organic carbon. All measured concentrations were in the standard range of the possible detection limit, accuracy was between 1 and 2%. Further measurement and processing details can be found at <http://acmelab.com>. The complete data set is shown in Table 1 supplementary material. Extract of this large data set is available in this text.

1.2.3. Samples

We sampled a complete section from Ordovician rocks to Permian successions in the area of La Paz (Northwest Bolivia; Fig. 1; Table 1 for the compilation of all GPS points). The GPS points are given below (see also Table 1) and help therefore to locate the samples easily on any satellite image. Paleogeographically, the region is called the Altiplano and Cordillera Oriental and the northern prolongation of the Argentinian Puna (Suárez Soruco, 2000). The Paleozoic record is represented with the formations: Amutara, Cancañiri, Uncía, Catavi, Vila, Belén, Sica, Colpacucho, Cumana, Kasa, Copacabana and Chutani (Fig. 2). Age constraints given here and short compilations of earlier descriptions are merged with findings in this study. Further information can be found in Suárez Soruco and Díaz Martínez (1996). For the Ordovician successions the data are compiled from Reimann Zumsprekel et al. (2015).

1.2.3.1. Ordovician. Coroico Formation: has been sampled along Ruta Nacional 3; thickness: more than 1500 m.

GPS point: S 16°16'04,4"; W 067°49'35,1"

Age: Darriwillian

Table 1

GPS data for the sample location of all here discussed formations. For their stratigraphic position and age please see section 'Methodology and Sampling', Fig. 2 and Supplementary Table 1.

FORMATION	GPS POINT	SAMPLES
Coroico	S 16°16'04,4"; W 067°49'35,1"	CORO
Amutara	S 16°16'25,1"; W 067°49'25,1"	AM
Cancañiri	S 16°19'15,3"; W 068°01'55,2"	CC
	S 16°19'21,8"; W 068°01'51,4"	CA2-CA7
	S 16°24'24,9"; W 068°02'56,6"	CAN4-CAN13
Uncía	S 16°25'03,0"; W 068°03'18,4"	UN
Catavi	S 16°25'47,7"; W 068°03'57,7"	CAT
Vila	S 16°44'05,50P; W 067°55'34,21P	VV
Belén	S 16°10'14,8"; W 068°49'42,0"	1X
	S 16°11'52,8"; W 068°32,58"	2X
	S 16°11'52,56"; W 068°49'24,66"	3X
	S 16°11'52,8"; W 068°49'32,58"	4x
Sica	S 16°58'42,26"; W 067°58'41,55"	SS
Colpacucho	S 16°58'57,32"; W 067°58'32,34"	CLP
Cumana	S 16°14'24,15"; W 068°51'31,3"	CU1-CU5
	S 16°14'14,4"; W 068°51'4,2"	CU6-CU9
Kasa	S 16°02'5,25"; W 069°09'24,15"	KS1-KS9
	S 16°02'5,25"; W 069°09'24,15"	KAS-I
Copacabana	S 16°14'17,47"; W 068°51'38,52"	COPA
Chutani	S 16°12'40,2"; W 068°50'25,8"	CH2-CH18
	S 16°12'48,0"; W 068°50'20,4"	CH20-CH30
	S 16°13'5,4"; W 068°49'56,4"	CH32-CH39

Main composition: The rocks are represented mainly by organic-rich shales and siltstones with very few sandstone intercalations. The rocks may have been slightly metamorphosed and are extremely reworked in terms of their heavy mineral composition. The rocks contain slumping features, load casts, abundant bioturbation and incomplete Bouma turbidite cycles. The base of the formation is unknown and the top is concordant to the Amutara Formation.

Amutara Formation: has been sampled along Ruta Nacional 3; thickness: more than 2000 m.

GPS point: S 16°16'25,1"; W 067°49'25,1"

Age: Katian-Sandbian

Main composition: The samples are very similar to those of the Coroico Formation but tend to show a higher frequency of coarser grained sandstones. The rocks show hummocky cross stratification and cross-bedding and as well bioturbation but turbidite related structures are not reported. The formation is concordant with the underlying Coroico Formation but discordant to the overlying Cancañiri Formation.

Outstanding for both Ordovician formations, is the fact that many samples are extremely enriched in chromium but chromite could not be identified. This is explained by sorting, as Reimann Zumsprekel et al. (2015) concentrated on studying the fraction larger than 65 µm.

1.2.3.2. Silurian. Cancañiri Formation: has been sampled along Ruta Nacional 3 in three main exposure sites; thickness: very variable (up to 1000 m), in this study 200–300 m.

GPS points: S 16°19'15,3"; W 068°01'55,2" (CC); S 16°19'21,8"; W 068°01'51,4" (CA2-CA7); S 16°24'24,9"; W 068°02'56,6" (CAN 4–13).

Age: Wenlock-Ludlow.

Main composition: The marine rocks in this outcrop area are dominated by dark grey to even black rare fine sandstones, massive siltstones and few shales s.s.. The shales are often black but do not contain organic components. One diamictite layer of c. 20 m thickness with large meter-sized blocks of granite and other clasts is strongly folded and faulted. Samples CC and CA have been sampled directly within (CC) and below this major diamictite layer. Samples CAN are collected further S along the main road where again diamictites are exposed, but with much smaller clast sizes (maximum 10 cm) and blueish to violet colored. The layers are intercalated with fine siltstones. The succession may represent deeper marine facies with dropstones. The formation is discordant to the

Table 2

Geochemical data of the Paleozoic successions with focus on typical values for alteration related interpretations. Please see for the complete data set [Supplementary Table 1](#). Green indicate Ordovician rocks, red Silurian samples, brown Devonian ones, blue those from Carboniferous successions and violet Permian strata. PPM = parts per million; % = weight percent; CIA, CIA* after Fedo et al. (1995) and therein.

element	CIA	CIA*	K/Cs	SiO2	CaO	Na2O	K2O	Cs	element	CIA	CIA*	K/Cs	SiO2	CaO	Na2O	K2O	Cs
unit				%	%	%	%	PPM	Unit				%	%	%	%	PPM
COROICO									SICA-SICA								
CORO 1	78	79	30,382	61.44	0.08	0.96	3.66	10.6	SS-1-a	65	68	5509	80.94	0.17	1.95	0.73	1.1
CORO 10	70	78	23,658	68.82	1.18	0.63	2.85	5.8	SS-13-a	71	74	3812	70.45	0.32	1.57	2.48	5.4
CORO 12 (AM)	78	79	5313	89.96	0.02	0.23	0.64	0.9	SS-14-a	67	70	4047	77.89	0.20	1.96	1.17	2.4
CORO 14 (AM)	82	93	2905	90.96	0.11	0.02	0.35	0.5	SS13	70	74	3923	70.96	0.31	1.59	2.41	5.1
CORO 16 (AM)	74	79	4732	91.24	0.12	0.36	0.57	0.7	SS14	67	69	5811	79.29	0.20	1.92	1.05	1.5
CORO 17 (AM)	77	82	7222	89.62	0.13	0.17	0.87	2.4	SS4	67	70	4483	78.22	0.22	1.87	1.35	2.5
AMUTARA									SS1	67	69	5155	78.73	0.17	1.99	1.18	1.9
AM 7	70	84	1328	96.52	0.14	0.03	0.16	0.4	SS15	66	68	4803	79.74	0.17	1.95	0.81	1.4
AM 9	53	54	6475	87.26	1.34	0.52	0.78	2.9	SS19	67	69	5147	78.77	0.14	1.95	0.93	1.5
AM 12	60	64	13,033	81.53	0.75	1.2	1.57	5.7	SS12	68	70	5271	76.84	0.28	1.85	1.27	2.0
AM 15	58	60	7388	83.58	0.85	1.48	0.89	2.2	SS2	67	69	5505	78.15	0.17	2.01	1.26	1.9
AM 20	62	67	1162	92.47	0.41	0.33	0.14	0.6	SS10	68	70	5188	77.14	0.19	1.93	1.25	2.0
CANCANIRI									SS5	70	73	4352	73.87	0.20	1.64	1.94	3.7
CC44	78	81	4178	56.3	0.24	0.52	4.63	9.2	SS11	70	73	3834	72.66	0.25	1.71	1.94	4.2
CC49	78	81	3943	60.92	0.26	0.45	3.99	8.4	COLLPACUCHO								
CC50	78	81	4170	55.73	0.38	0.52	4.32	8.6	CLP-7b	66	70	5759	77.17	0.24	1.98	1.11	1.6
CA2	78	81	4171	61.52	0.25	0.39	4.02	8	CLP-5b	68	72	5060	76.27	0.26	1.88	1.28	2.1
CA8	73	81	3190	59.15	1.21	0.55	3.92	10.2	CLP-12 b	70	74	5088	69.79	0.28	2.00	1.90	3.1
CA9	77	80	5048	56.26	0.35	0.71	4.5	7.4	CLP2b	68	70	6779	77.26	0.16	1.98	0.98	1.2
CA1	78	81	5053	64.49	0.19	0.43	3.47	5.7	CLP13b	68	73	7416	74.50	0.25	1.97	1.34	1.5
CA6	78	81	3693	61.09	0.26	0.46	3.96	8.9	CLP9b	60	64	6960	76.19	1.02	2.05	1.09	1.3
CA7	78	81	3847	61.21	0.27	0.51	3.8	8.2	CLP1	67	69	6018	78.92	0.16	1.96	0.87	1.2
CAN4	78	82	2555	64.08	0.23	0.56	3.54	11.5	CLP12b	69	72	5811	73.35	0.26	2.01	1.47	2.1
CAN5	78	81	3477	66.23	0.23	0.4	3.56	8.5	CLP15	67	71	5010	73.67	0.39	1.99	1.69	2.8
CAN8	77	81	4189	59.2	0.31	0.4	4.34	8.6	CLP5	69	73	4892	72.42	0.26	1.87	1.65	2.8
CAN9	78	81	4133	55.9	0.25	0.47	4.83	9.7	CLP3b	65	69	5257	79.95	0.21	2.04	0.95	1.5
CAN11	77	80	5557	65.79	0.19	0.34	3.95	5.9	CLP7b	65	68	6433	79.54	0.21	2.07	0.93	1.2
CAN12	75	78	4480	68.22	0.23	0.67	3.67	6.8	CUMANÁ								
CAN13	76	79	4072	76.07	0.23	0.43	2.6	5.3	CU1	61	62	9618	76.04	0.20	2.14	3.36	2.9
CAN10	68	71	4519	89.55	0.1	0.82	0.49	0.9	CU2	62	64	10,360	76.30	0.25	2.07	3.12	2.5
CAN6	71	74	5534	85.5	0.15	0.93	0.8	1.2	CU4	60	61	9477	72.37	0.52	2.17	4.11	3.6
CAN7	67	69	5534	88.25	0.11	1.12	0.8	1.2	CU5	58	60	11,665	78.65	0.19	2.41	2.67	1.9
UNCIA									CU6-2	57	58	8527	85.72	0.06	2.48	1.13	1.1
UN1	79	83	2192	66.77	0.24	0.58	2.35	8.9	CU6-3	63	64	9546	83.12	0.10	0.90	2.99	2.6
UN2-A	74	77	6235	60.92	0.37	1.16	3.23	4.3	CU6-4	61	62	6199	81.47	0.15	0.87	3.51	4.7
UN2	85	90	2100	76.59	0.18	0.13	0.86	3.4	CU6-5	62	64	11,185	84.67	0.11	0.87	2.56	1.9
UN3	78	83	1833	62.34	0.33	0.77	3.18	14.4	CU7-1	63	64	6708	77.68	0.20	1.94	2.99	3.7
UN4	78	83	1676	62.72	0.34	0.69	3.17	15.7	CU7-2	64	66	10,344	76.74	0.22	1.42	3.24	2.6
UN6	78	84	1574	61.39	0.34	0.73	3.47	18.3	CU8	62	63	9719	85.31	0.09	0.78	2.81	2.4
UN7	81	86	1766	77.11	0.09	0.44	1.34	6.3	CU9	64	66	5969	76.60	0.20	1.87	3.02	4.2
UN8	78	84	2141	63.24	0.23	0.72	3.25	12.6	KASA								
UN9	78	82	1933	62.94	0.22	0.78	3.54	15.2	KAS-1-1	58	58	21,108	70.39	0.39	5.30	1.78	0.7
UN10	83	89	2551	71.58	0.28	0.18	1.26	4.1	KAS-1-2	56	56	31,129	69.97	0.58	6.10	2.25	0.6
UN13	77	82	1474	79.83	0.12	0.74	1.03	5.8	KS1	55	55	31,544	87.52	0.09	1.65	1.90	0.5
UN15	77	82	1950	69.74	0.21	0.75	2.49	10.6	KS2	59	60	7678	79.44	0.20	2.44	2.59	2.8
UN16	75	80	2719	81.94	0.25	0.59	0.95	2.9	KS3	64	67	19,092	91.48	0.06	0.57	1.38	0.6
UN12	76	83	2011	68.99	0.48	0.69	2.35	9.7	KS5	62	64	12,452	85.07	0.09	1.82	1.65	1.1
UN11	79	85	1937	71.88	0.21	0.60	1.82	7.8	KS4	62	63	16,376	76.53	0.26	2.41	2.17	1.1
UN14	77	83	1737	61.67	0.24	0.83	3.85	18.4	KS6	62	65	21,251	91.47	0.03	0.75	1.28	0.5
CATAVI									KS7	61	64	19,092	92.54	0.02	0.66	1.15	0.5
CAT3	77	82	1120	58.11	0.17	0.59	5.26	39	KS8	65	69	11,345	88.38	0.05	0.40	1.23	0.9

(continued on next page)

Table 2 (continued)

element	CIA	CIA*	K/Cs	SiO2	CaO	Na2O	K2O	Cs	element	CIA	CIA*	K/Cs	SiO2	CaO	Na2O	K2O	Cs
CAT4	67	69	1969	88.23	0.11	1.31	0.83	3.5	KS9	59	62	17,847	90.36	0.05	1.53	0.86	0.4
CAT5	77	82	1110	59.25	0.17	0.74	4.2	31.4	COPACABANA								
CAT6	75	78	1064	71.35	0.17	1.03	2.59	20.2	COPA1a	21	26	6583	43.90	17.99	0.43	4.52	5.7
CAT11	76	89	1136	48.67	0.42	0.23	5.13	37.5	COPA2	67	68	4257	71.54	0.49	0.73	4.00	7.8
CAT12	83	85	1649	84.46	0.07	0.05	1.49	7.5	COPA3	23	28	6934	47.88	15.68	3.12	1.42	1.7
CAT13	75	80	1178	63.17	0.29	0.73	4.13	29.1	COPA4	66	68	3292	73.53	0.50	0.78	3.45	8.7
CAT14	64	70	1516	81.72	0.35	1.57	1.26	6.9	COPA6	22	27	5594	44.15	17.70	2.92	1.55	2.3
CAT15	75	89	1309	54.22	0.42	0.23	4.73	30	COPA7	13	17	4308	37.37	25.61	0.31	1.92	3.7
CAT19	77	80	1138	59.41	0.11	0.78	4.43	32.3	COPA8a	64	67	4783	62.78	1.28	0.14	5.82	10.1
CAT20	71	75	1085	72.76	0.57	0.99	2.51	19.2	COPA8b	67	70	4519	64.55	0.71	0.09	5.77	10.6
CAT21	77	84	1075	60.01	0.29	0.36	4.7	36.3	COPA10	25	31	7143	52.09	14.04	1.03	3.27	3.8
CAT22	82	85	1474	87.93	0.03	0.07	1.19	6.7	COPA11	66	69	6505	66.25	0.78	0.87	3.84	4.9
CAT8	68	74	1331	77.75	0.45	1.10	1.62	10.1	COPA13	57	61	6398	52.47	3.35	0.03	8.71	11.3
CAT9	75	79	1101	63.84	0.17	0.90	4.06	30.6	COPA14	67	70	3743	68.09	0.52	0.12	5.14	11.4
CAT17	74	77	1235	67.78	0.16	1.04	3.48	23.4	CUCO1	60	62	8788	68.98	0.41	1.88	4.87	4.6
CAT18	71	74	1395	75.01	0.23	1.41	2.10	12.5	CHUTANI								
VILA-VILA									CH-1	2	3	4981	70.36	14.57	0.06	0.12	0.2
VV-1	64	78	7290	81.10	0.78	0.12	2.02	2.3	CH-4	1	1	1660	81.84	9.41	0.03	0.02	0.1
VV-5	71	81	7748	80.31	0.33	0.20	2.24	2.4	CH-7	32	36	18,816	54.49	8.53	3.37	3.40	1.5
VV-12	68	73	7782	90.43	0.22	0.07	1.50	1.6	CH-8	34	39	20,144	57.91	7.12	2.46	3.64	1.5
VV7	70	79	8384	82.27	0.41	0.09	2.02	2.0	CH-11	46	48	62,534	62.27	2.58	6.05	2.26	0.3
VV6	70	80	7810	81.85	0.34	0.13	2.07	2.2	CH-12	46	48	60,182	63.57	3.08	4.86	2.90	0.4
VV2	62	76	8024	80.76	0.93	0.10	2.03	2.1	CH-13	52	53	72,219	67.31	0.60	5.57	2.61	0.3
VV13	65	71	9269	89.74	0.38	0.08	1.34	1.2	CH-16	35	41	41,782	64.37	6.70	5.71	1.51	0.3
VV15	71	79	7163	79.39	0.29	0.30	2.33	2.7	CH-18	28	32	115,384	55.12	11.69	6.10	1.39	0.1
VV16	74	78	2652	57.60	0.42	1.16	4.09	12.8	CH-20	43	60	13,904	70.33	3.55	2.63	2.01	1.2
VV11	72	76	12,867	90.99	0.06	0.09	1.24	0.8	CH-21	48	61	14,997	68.37	2.63	2.57	2.71	1.5
VV8	71	78	8376	81.54	0.36	0.10	2.22	2.2	CH-22	47	61	13,428	68.53	2.91	2.54	2.75	1.7
BELEN									CH-25	48	59	15,918	64.39	2.93	3.91	3.26	1.7
1 × 4GS	69	72	6087	73.83	0.69	0.62	1.54	2.1	CH-29	25	53	19,577	71.42	6.76	1.18	2.83	1.2
1 × 1GS	57	58	7388	86.93	1.94	0.01	0.89	1	CH-30	24	54	31,619	56.05	11.06	1.73	4.19	1.1
1 × 2GS	76	79	5989	88.71	0.28	0.01	1.01	1.4	CH-32	32	50	26,445	52.65	8.06	5.02	4.46	1.4
1 × 3GS	65	67	6122	84.48	0.38	1.09	1.18	1.6	CH-35	45	51	18,495	58.76	2.15	4.82	5.57	2.5
2 × 2GS	74	76	3161	71.63	0.77	0.18	2.97	7.8	CH-36	9	55	14,388	42.38	25.52	0.68	2.60	1.5
2 × 4GS	72	74	3605	75.94	0.7	0.55	1.52	3.5	CH-38	7	56	13,282	38.08	28.50	0.35	2.40	1.5
2 × 1GS	73	74	2934	69.49	0.81	0.44	3.11	8.8	CH-39	9	53	18,885	41.38	26.10	0.93	2.73	1.2
2 × 3GS	76	83	4278	84.82	0.37	0.25	0.67	1.3									
3 × 4GS	82	84	6226	85.68	0.16	0.01	1.05	1.4									
3 × 1GS	76	76	3430	72.95	0.52	0.06	3.76	9.1									
3 × 2GS	82	85	4590	87.49	0.14	0.01	0.94	1.7									
3 × 3GS	80	81	4119	72.68	0.35	0.04	2.58	5.2									
4 × 1GS	70	72	3792	77.04	0.66	0.72	1.69	3.7									
4 × 2GS	76	79	3203	69.4	0.5	0.08	3.01	7.8									
4 × 4GS	75	75	2705	69.07	0.66	0.05	4.53	13.9									
4 × 3GS	70	72	3593	71.67	0.87	0.5	3.03	7									

underlying Amutara Formation and concordant to the overlying Uncía Formation.

Uncía Formation: has been sampled along Ruta Nacional 3; thickness: more than 2000 m.

GPS point: S 16° 25' 03,0"; W 068° 03' 18,4"

Age: Wenlock-Ludlow.

Main composition: The marine rocks are brown to grey-green colored, very homogeneous and dominated by fine sandstones to siltstones. Shales are not significant in their abundance. There are no sedimentary structures pointing to a turbidite environment, rather a shallow marine facies. The formation is concordant to the underlying Uncía Formation and overlying Catavi Formation.

Catavi Formation: has been sampled along Ruta Nacional 3; thickness 2000 m.

GPS point: S 16° 25' 47,7"; W 068° 03' 57,7"

Age: Ludlow-Pridoli

Main composition: The marine rocks are light green to brown colored, homogeneous and mainly medium to fine grained sandstones with siltstones and few shales intercalated. The successions do not show any sedimentary structure pointing to turbidite deposition, but ripple marks and ichnological features. The formation is concordant to the underlying Uncía Formation and overlying Vila Formation.

1.2.3.3. *Devonian*. Vila Formation: has been sampled in the folded area of Huarina; thickness 200–1900 m.

GPS point: S 16° 44' 05,50P; W 067° 55' 34,21P

Age: Lower Devonian.

Main composition: The marine rocks are light brown to yellow colored, mainly medium to fine grained sandstones, shales are rare and deposited in a shallow marine environment. The formation is concordant to the underlying Catavi Formation and overlying Belén Formation.

Belén Formation: has been sampled along Ruta Nacional 2 5–10 km N of Tiquina in four different outcrops; thickness: up to 2500 m.

GPS points: S 16° 10' 14,8"; W 068° 49' 42,0" (1X samples); S 16° 11' 52,8"; W 068° 32,58" (2X); S 16° 11' 52,56"; W 068° 49' 24,66" (3X); S 16° 11' 52,8"; W 068° 49' 32,58" (4X).

Age: Upper Pragian-Emsian

Main composition: The marine rocks are brown to dark green and mainly sandstones with intercalated siltstones and brown shales. Sedimentary structures show partly incomplete Bouma turbidite cycles and cross bedding. The formation is concordant to the underlying Vila Formation and overlying Sica Formation.

Sica Formation: has been sampled close to the highway La Paz-Oruro at El Tholar; thickness: up to 1000 m.

GPS point: S 16° 58' 42,26"; W 067° 58' 41,55".

Age: Lower to Middle Devonian.

Main composition: The rocks are light brown to grey and are dominated by sandstones, but elsewhere higher shale content can be observed. The rocks are homogeneous banked and do not show any sedimentary structures besides cross bedding and are interpreted to be deposited in a shallow marine environment according to the fossil content. The formation is concordant to the underlying Belén Formation and overlying Collpacucho Formation.

Collpacucho Formation: has been sampled close to the highway La Paz-Oruro at El Tholar; thickness: up to 2000 m.

GPS point: S 16° 58' 57,32"; W 067° 58' 32,34".

Age: Givetian-Frasnian

Main composition: The rocks are grey to dark greenish and show intercalations of siltstones and sandstones. Within the formation cross bedding, load casts, ripple marks and small-scaled channels are observable, Bouma sequences are absent and the rocks may be deposited in a shallow marine environment. The formation is concordant to the underlying Sica Formation but pseudoconcordant to the overlying Cumaná Formation.

1.2.4. *Cumaná Formation*: has been sampled at huajllani in two areas; thickness: up to 120 m

GPS point: S 16° 14' 24,15"; W 068° 51' 31,3" (CU1-5); S 16° 14' 14,4"; W 068° 51' 4,2" (CU6-9).

Age: Upper Devonian-Mississippian

Main composition: The rocks are red to dark orange colored and characterized by intercalation of hard sandstones, siltstones, few light colored shales and thin layers of diamictites. In the sampling area these layers are rare and not thicker than 1 m with clast sizes below 10 cm, mostly of volcanic and plutonic origin. Cross stratifications have been observed but no other sedimentary structures. The formation is discordant and erosive to the underlying Collpacucho Formation but concordant to the overlying Kasa Formation.

1.2.4.1. *Carboniferous*. Kasa Formation: has been sampled above the Cumaná Formation at Huajllani and on the Isla del Sol; thickness: up to 900 m.

GPS point: S 16° 02' 5,25"; W 069° 09' 24,15" (KS1-9); S 16° 02' 5,25"; W 069° 09' 24,15" (KAS-I).

Age: Lower Carboniferous.

Main composition: The rocks are red and partly orange colored, relatively friable, and characterized by cross stratification. Few and thin layers (<30 cm) of diamictites with small clast sizes (<5 cm) and siltstones are deposited. There are no clear parameter to define a continental or marine environment for this succession. The formation is concordant to the underlying Cumaná Formation and overlying Siripaca Formation (not sampled in this study).

Copacabana Formation: has been sampled 2 Km S of San Pablo de Tiquina; thickness: 400–750 m.

GPS point: S 16° 14' 17,47"; W 068° 51' 38,52".

Age: Upper Carboniferous-Cisuralian

Main composition: The marine formation is composed of thick carbonate successions intercalated with marls, siltstones and few sandstones as well as green ash layers. Here, we sampled only clastic rocks and marls, which are yellow, green and reddish colored. Sedimentary structures in the non-carbonate sections are scarce with mainly bioturbations. The facies can be described as shallow marine. The formation is concordant to the underlying Yaurichambi Formation (30 m thickness, not sampled in this study) and overlying Chutani Formation.

1.2.4.2. *Permian*. Chutani Formation: has been sampled along Ruta Nacional 2, 4 km N of Tiquina in three exposures; thickness: up to 400 m.

GPS point: S 16° 12' 40,2"; W 068° 50' 25,8" (CH2 – CH18); S 16° 12' 48,0"; W 068° 50' 20,4" (CH20 – CH30); S 16° 13' 5,4"; W 068° 49' 56,4" (CH-32- CH-39).

Age: Guadalupian-Lower Triassic.

Main composition: The formation is composed of dolomites, silt and sandstones, marls and few epiclastic layers. The latter are dark brown while the clastic rocks are light orange to greenish. The fossil content points to a marine deposition but may also be partly continental with occurrence of plant material. The formation is concordant to the underlying Copacabana Formation and overlying Tiquina Formation.

2. Results

2.1. Petrography

The rocks of the Coroico and Amutara formations have been studied in detail by Reimann Zumsprekel et al. (2015). The former are characterized by mainly organic-rich shales with a significant amount of secondary chlorite and quartz. The Amutara Formation contains arenites which enabled feasible point counting (Reimann Zumsprekel et al., 2015). The authors determined well sorted rocks with a clear dominance of quartz (>90%), few feldspar, and then alkalifeldspar and accessory lithoclasts of mainly sedimentary origin. Although highly

compositionally mature, the rocks contain up to 20% matrix.

The overlying successions of the Cancañiri Formation varies lithologically within exposures in Bolivia (Suárez Soruco and Díaz Martínez, 1996). In the study area the formation is characterized by mainly very fine grains within the few sandstones and siltstones at the exposure La Cumbre (Fig. 3a). The black shales are composed of quartz, alkalifeldspar and illite (identified, here and below, by X-ray diffraction or

electron microscopy coupled with energy dispersive spectrometry) as well as chlorite and iron-oxide. Although the shales are black, organic matter is not abundant with total carbon far below 0,3 wt percent (wt.%) and total organic carbon mostly far below 0,22 wt% (Supplementary Table 1). The siltstones are homogeneous with a high amount of opaque phases and pyrite but dominated by quartz, illite and few alkalifeldspar (Fig. 3a–b). The sandstones show mainly angular larger clasts of quartz,

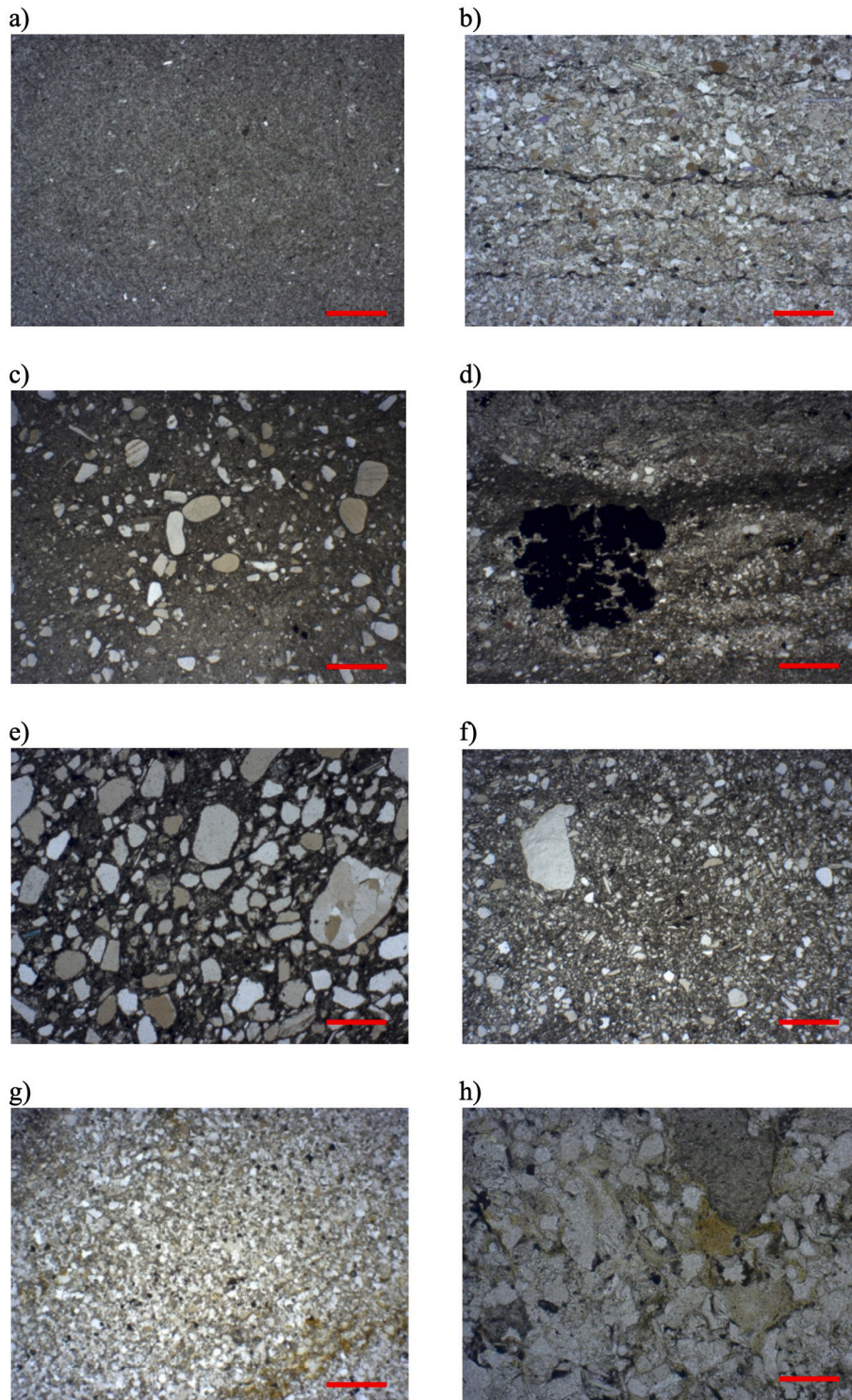


Fig. 3. Petrographic micrographs. a) Siltstone Cancañiri Formation; bar = 160 µm; b) detail sandstone Cancañiri Formation; bar = 80 µm; c) diamictite Cancañiri Formation La Cumbre; bar = 300 µm; d) detail siltstone Cancañiri Formation La Cumbre; bar = 80 µm; e) diamictite Cancañiri Formation dam; bar = 160 µm; f) detail diamictite Cancañiri Formation dam; bar = 80 µm; g) fine sandstone Uncía Formation; bar = 300 µm; h) detail sandstone Uncía Formation; bar = 80 µm.

poor sorting and diagenetic formed thin layers of clay and iron-oxide or other opaque phases (Fig. 3b). The diamictite are composed of fine sandy to silty matrix with quartz, few alkalifeldspar, illite, chlorite and muscovite (Fig. 3c). The clasts are mostly subrounded to rounded if they are larger. Few rounded feldspar clasts have been observed and rounded sedimentary lithoclasts, composed of rounded and angular grains (Fig. 3c). Finer grained intercalations within the diamictites show high amounts of clay and massive pyrite in nests or scattered in the matrix (Fig. 3d). Few kilometer afar, the Cancañiri Formation shows several thin diamictite layers with a very fine sandy matrix and few large clasts

scattered with the matrix (Fig. 3 e-f). These clasts are mostly quartz or metamorphic lithoclasts, subrounded and few well rounded. Smaller clasts are mostly subangular to angular. The diamictites are matrix-supported. The matrix is dark, clay- and iron-oxide rich and contains also opaque phases but no organic carbon (see Supplementary Table 1). Other layers are composed of a poorly sorted matrix with rounded but mainly angular grains of mostly quartz origin with few alkalifeldspar (Fig. 3f). Opaque phases, illite and mica are other minerals composing the matrix. Few large, angular mainly quartz clasts are scattered in this sandy to silty matrix. Shales are similar to those from La

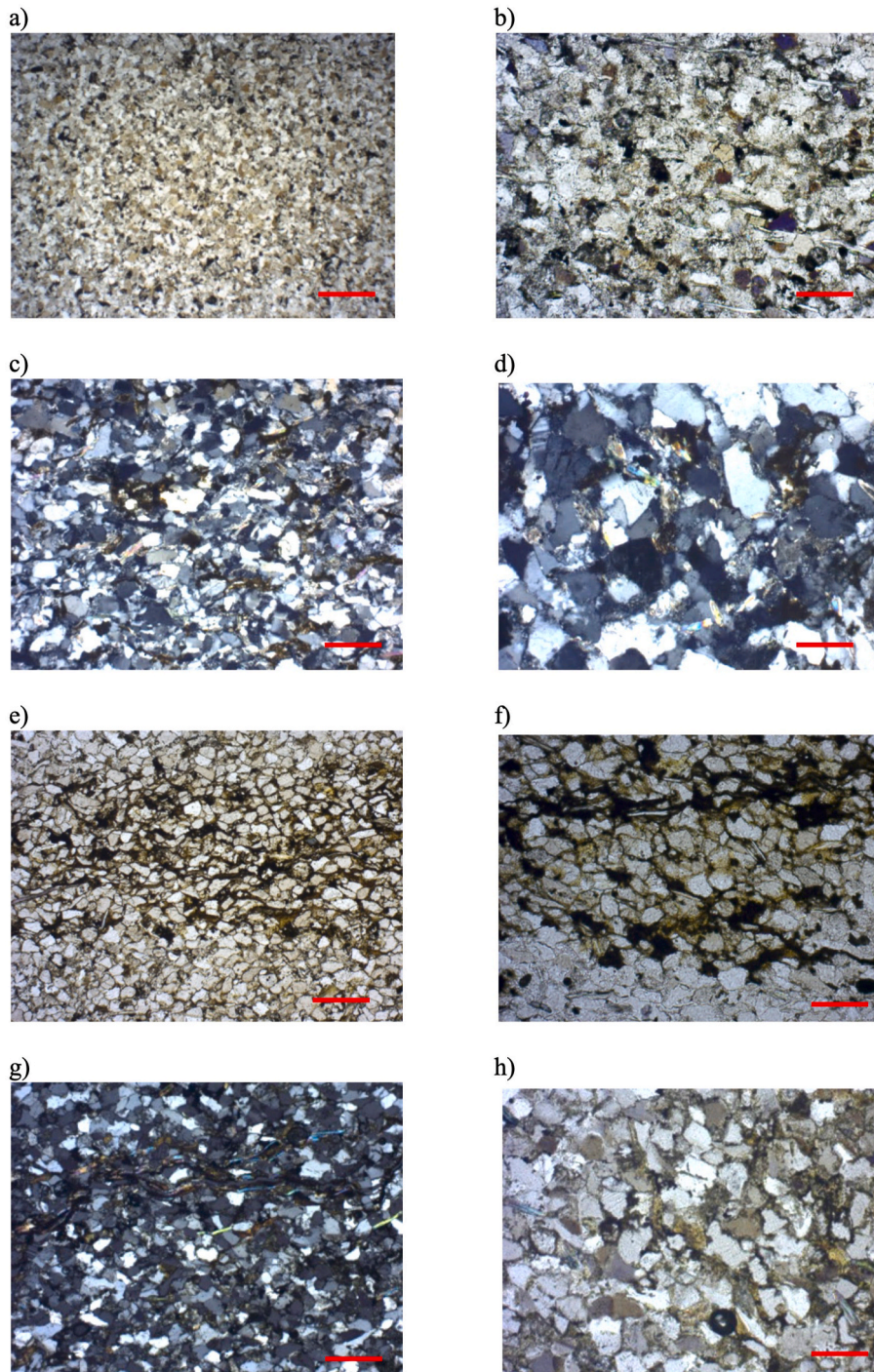


Fig. 4. Petrographic micrographs. a) Fine sandstone Catavi Formation; bar = 300 μm ; b) detail sandstone Catavi Formation; bar = 80 μm ; c) fine sandstone Vila Formation; bar = 160 μm ; d) detail sandstone Vila Formation; bar = 80 μm ; e) fine sandstone Belén Formation; bar = 300 μm ; f) detail sandstone Belén Formation; bar = 80 μm ; g) fine sandstone Sica Formation; bar = 160 μm ; h) detail sandstone Sica Formation; bar = 80 μm .

Cumbre.

Overlying rocks of the Unciá Formation are dominated by quartz, with few alkalifeldspar, significant amounts of muscovite, illite and opaque phases. Chlorite is less rather accessory. The rocks are bimodally sorted and mostly subangular to angular grains occur with few rounded components (Fig. 3g–h). The decay of lithoclasts may have formed the up to 10% (pseudo-)matrix (Fig. 3h). The successions of the Catavi Formation is rather similar but contains even least rounded grains, more opaque phases and muscovite and seems slightly better sorted (Fig. 4a–b).

Devonian deposits, besides the Cumaná Formation, are represented by the Vila-Vila, Belén, Sica-Sica and Collpacucho formations, from old to young (Figs. 4 and 5). The rocks are relatively similar petrographically and can be described as mainly composed of sub-rounded to sub-angular grains, while the latter clearly dominate. Rounded clasts are nearly absent while angular ones abundant. Quartz is by far the most abundant mineral, followed by alkalifeldspar and few plagioclases. Muscovite and illite, as well as iron-oxides are common. The Vila Formation shows less matrix content (Fig. 4c–d), the rocks of the Belén Formation are enriched in matrix and clay minerals compared to the

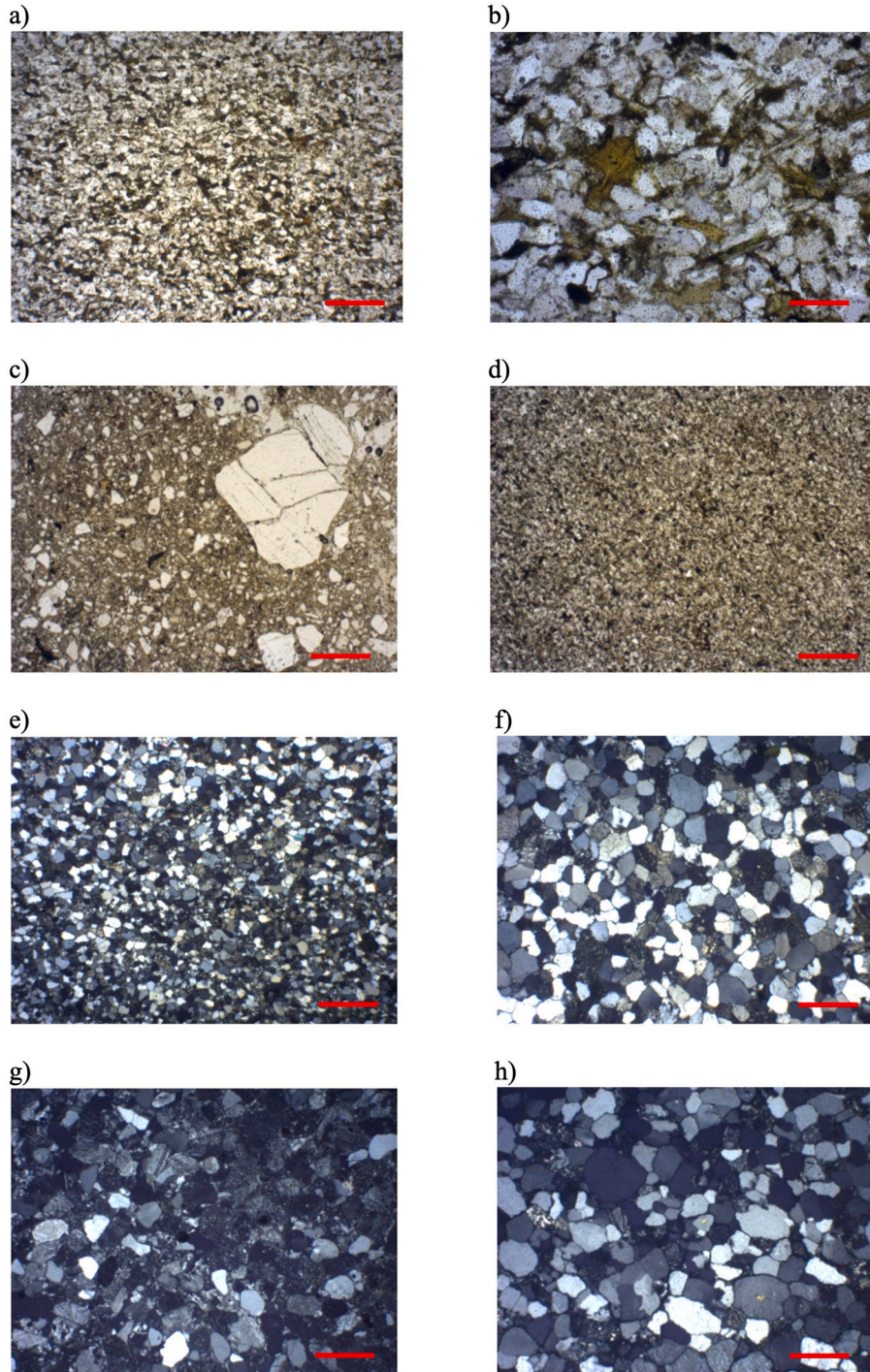


Fig. 5. Petrographic micrographs. a) Sandstone Collpacucho Formation; bar = 160 μm; b) detail sandstone Collpacucho Formation; bar = 80 μm; c) diamictite Cumaná Formation; bar = 300 μm; d) sandstone Cumaná Formation; bar = 300 μm; e) graded sandstone Kasa Formation; bar = 160 μm; f) detail sandstone Kasa Formation; bar = 300 μm; g) feldspar-rich sandstone Kasa Formation Isla del Sol; bar = 300 μm; h) sandstone Kasa Formation Isla del Sol; bar = 160 μm.

other Devonian deposits (Fig. 4e–f). The amount of muscovite rises within the Sica Formation rocks (Fig. 4g–h), while those of the Collpaucucho Formation are very large (Fig. 5a–b).

The Cumaná Formation hosts, as mentioned, diamictites and is subject of the hypothesis of a glacial event during the Devonian in the Central Andes (Díaz Martínez and Isaacson, 1994). Its depositional age straddles the Devonian-Carboniferous boundary and the sample here collected show similarities to the diamictites of the Cancañiri Formation. A sandy to silty matrix hosts angular to sub-rounded clasts often composed of quartz (Fig. 5c). Nevertheless, the mineralogical composition differs not strongly from the described Devonian above in the main abundant silt to sandstones, but contain smaller grainsizes with higher amounts of clays and opaque minerals (Fig. 5d).

The transition at Huajllani to the overlying Kasa Formation is marked by a color change from orange to red, culminating in even red beds. The red sandstone succession are moderately sorted and grains are rounded to subangular. The rocks are dominated by quartz and alkali-feldspar with few plagioclase (Fig. 5e–f). Muscovite is only accessory, so are opaque phases or clay minerals. Lithoclasts are mostly of meta-sedimentary or high-grade metamorphic origin (polycrystalline quartz clasts). Matrix is nearly absent in these samples. At the outcrops on the Isla del Sol (Supplementary Table 1), the rocks contain slightly higher amount of matrix with a notable amount of lithoclasts (metasedimentary

and sedimentary; Fig. 5g–h). The samples are moderately sorted and grains are from rounded to angular. Some quartz grains can be interpreted as having embayments typical for quartz of volcanic origin (Fig. 5h).

Concordant follows the mainly carbonate containing Copacabana Formation. The clastic lithologies are mostly dominated by quartz, often angular to subangular, very few rounded components are deposited (Fig. 6a–b). Mica is again, abundant, so are clay minerals, opaque phases and chlorite, which may be reworked volcanic detritus as volcanic ashes are abundant in the successions and dated (Hamilton et al., 2016). Alkali-feldspar is common but plagioclase nearly absent. Matrix content can be up to 15%. Often larger shell fragments are deposited within clastic successions or the rocks grade into marls (Fig. 6b).

Finally, the uppermost succession within the Paleozoic is the Chutani Formation, with thick carbonate layers. The clastic rocks and marls contain a wide range of grain forms, from rounded to angular and reflect poor mixing. Quartz is still the dominant phase together with alkali-feldspar and common plagioclase as well as polycrystalline quartz, opaque phases and clays (Fig. 6c–e). In some fine grained sandstones to siltstones, often large fragments occur with a black matrix (Fig. 6d). In those lithotypes the grains are more angular (Fig. 6e). Clay-rich layers may be ash deposits or epiclastic rocks with often v-shaped components filled with platy quartz (Fig. 6f). These may have been fossil shells or

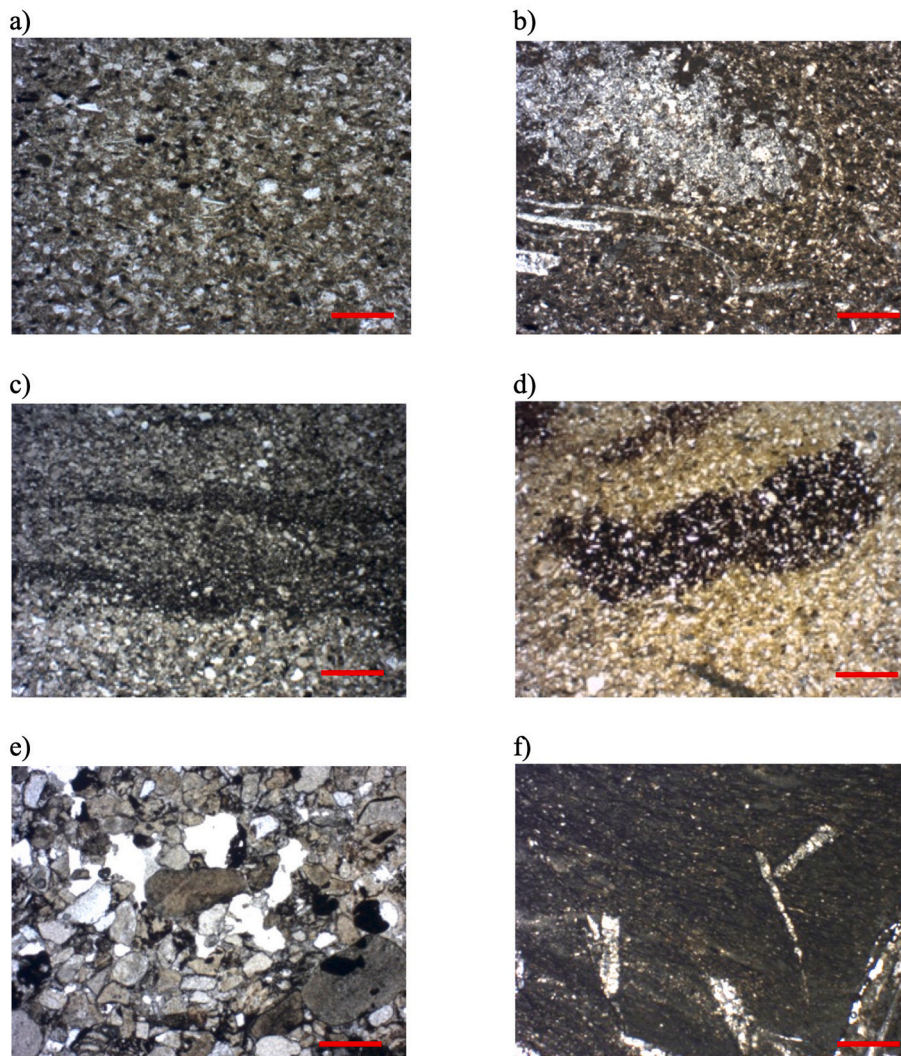


Fig. 6. Petrographic micrographs. a) mica-rich sandstone Copacabana Formation; bar = 80 μm ; b) clay-rich sandstone Copacabana Formation with abundant shells; bar = 160 μm ; c) graded sandstone Chutani Formation; bar = 300 μm ; d) clay-rich fragment in siltstone Chutani Formation; bar = 160 μm ; e) sandstone Chutani Formation; bar = 300 μm ; f) detail possible volcanoclastic rock with funnel-shaped areas filled with platy quartz; bar = 160 μm .

evaporite crystals – however, the origin of those is still unknown.

2.1.1. Compilation of the petrography

Throughout the entire stratigraphy we cannot observe significant compositional changes, which would point to a change of the paleotectonic setting or the introduction of a different source component. Significant compositional changes throughout the Paleozoic are only in few stratigraphic positions developed. The Amutara Formation is represented by rounded quartz dominated, well sorted rocks (Reimann Zumsprekel et al., 2015). The Silurian rocks show, in turn, only sporadically well rounded clasts and are characterized by moderate sorting, subrounded to subangular grains, abundant opaque phases, illite and pyrite. Alkalifeldspar is common. In the shallow marine successions, stratigraphically above the diamictite bearing Cancañiri Formation, muscovite is a common feature within the petrography. During the Devonian the characteristics do not change significantly but shales are rare and diamictites are absent. The diamictites of the Upper Devonian Cumaná Formation resemble those in the Silurian Cancañiri Formation (Figs. 3d and 5c). The rocks of the Cumaná Formation contain much less muscovite and have a higher amount of matrix, while siltstones and fine sandstones are comparable with the older Devonian successions and to the overlying clastic rocks of the Copacabana Formation. However, various clastic dominated rocks of the Copacabana Formation show possible reworked volcanic detritus and shell fragments with differences in regard of the abundance of carbonate and fossil fragments (Fig. 6b). Finally, the Permian to Lower Triassic Chutani Formation is slightly different with higher amounts of rounded clasts and abundance of possible volcanic detritus, even possible ash horizons or epiclastites.

Geochemistry.

2.2. Major elements and alteration

Ordovician quartz-arenites are mostly enriched in silica and depleted in most of the other major elements. The few shales show a typical upper continental crust composition (UCC after McLennan et al., 2006; Supplementary Table 1). CIA (chemical index of alteration after Nesbitt and Young, 1982) values are reported, together with the other geochemical data, by Riemann Reimann Zumsprekel et al. (2015). The CIA is generally high and point to strongly altered rocks. Some samples of the Amutara Formation show lower values mainly affected by increased carbonate content. Two samples of the Coroico Formation, the shales CORO 1 and CORO10, are extremely enriched in K_2O , while the K/Cs ratios for the other samples are between 7220 and 2905. K/Cs ratios are mostly very high pointing to a low weathering; however, this is controlled by geochemical depletion as a consequence of the high silica content and therefore only extremely low Cs concentrations (Table 1; Fig. 7).

The Silurian rocks are very different with a generally lower silica content and increased Al_2O_3 , K_2O , MgO and Fe_2O_{3T} concentrations caused by higher amounts of clays and phyllosilicates. Still low (below typical UCC) are the concentrations in CaO , Na_2O , P_2O_5 and MnO . TiO_2 varies strongly, with low values in silica richer samples (70–85 wt%; wt % indicates weight percent) and higher values in those with silica comparable to typical UCC. CIA values are within the Silurian formations generally still high with only few samples below 70 (Table 1). This correlates with low K/Cs ratios (Fig. 7; Table 1) and shows a clear trend from higher values between 3000 and 6000 (below typical UCC) for the Cancañiri Formation, followed by values even lower than typical PAAS (Post-Archean Average shale after Taylor and McLennan, 1985) stratigraphically up.

Devonian successions, excluding the Cumaná Formation, are geochemically relatively homogeneous. Most of the samples contain between 70 and 80% SiO_2 and are slightly depleted in all other major elements compared to typical UCC. Fe_2O_{3T} and TiO_2 are, in turn, slightly more abundant than in typical UCC. CIA are significantly lower than in

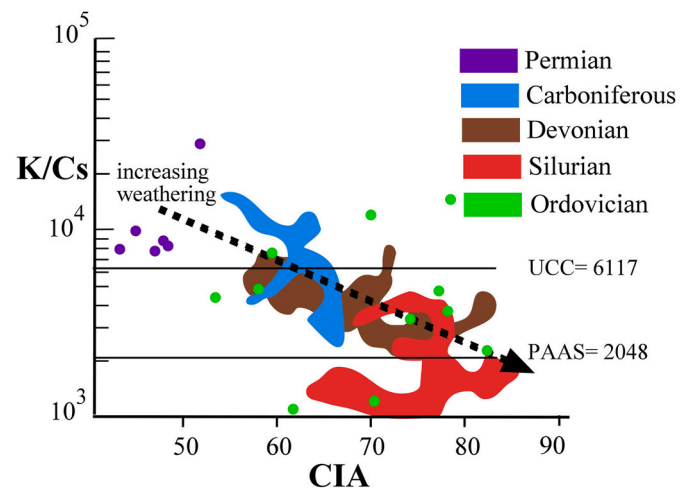


Fig. 7. CIA (Chemical Index of Alteration; after Nesbitt and Young, 1982) versus K/Cs to estimate alteration and weathering (after McLennan et al., 1993). Values below typical shale (after Taylor and McLennan, 1985) indicate strong weathering and should correlate with high CIA values in groups, the other orientation is the K/Cs of typical Upper continental crust composition (after McLennan et al., 2006).

the rocks of the Silurian and Ordovician, with values between 60 and 70 (Table 1; Fig. 7). This correlates very well with increased K/Cs ratios mostly above 3000 (Table 1; Fig. 7).

The Cumaná Formation, suspect of being related to a glacial environment (Díaz Martínez and Isaacson, 1994), shows a larger variability in all major elements but definitely lower Fe_2O_{3T} and TiO_2 values than the other Devonian rocks (Table 1). CIA values are low which also correlated with higher K/Cs ratios (Table 1). Cs concentrations are robust low and not related to depletion as the rocks are not enriched in silica, besides one sample, hence this trend may be a realistic reflection of the weathering.

The trend of low CIA values in rocks - devoid of large amounts of carbonate (CaO , see Table 1) - and high K/Cs ratios continues in the Lower Carboniferous Kasa Formation (Table 1; Fig. 7). Rocks are, however, enriched in quartz and therefore contain often above 85 wt% SiO_2 concentrations which diluted major elements. Siltstones and shales are enriched in Na_2O , Al_2O_3 obviously, but rarely in TiO_2 or Fe_2O_{3T} (Table 1; Fig. 7). The overlying Copacabana Formation contains marls (14–25 wt% CaO) and sandstones. The latter contain typical UCC. CIA values are difficult to interpret and within the sandstones between 60 and 70 with K/Cs ratios from 3700 to 7150 (Table 1; Fig. 7).

The Permo-Triassic successions of the Chutani Formation carries in all clastic dominated samples significant concentrations of CaO from 2 to 12 wt% while three marls have higher CaO concentrations (Table 1). In the clastic dominated rocks, the abundances of the major elements are comparable to typical UCC with strong variations within the concentrations of TiO_2 from 0,01 wt% to 0,73 wt%.

Ratios of Nb/Y and Zr/Ti (Winchester and Floyd, 1977) are frequently used to determine the general trace element composition of clastic rocks (e.g. Fralick, 2003; Lacassie et al., 2006), knowing that major element ratios or plots are not feasible (e.g. Armstrong-Altrin and Verma, 2005). Fig. 8 splits, for the deposited detrital mixes, samples with trends towards an overall alkaline composition, felsic or basaltic. Zr and Ti refer mostly to ultrastable heavy minerals, zircon and rutile respectively, while Nb/Y indicate a dominantly alkaline composition with increased Nb/Y ratios versus a calc-alkaline compositions (Fig. 8).

The Ordovician rocks are variable in terms of their Zr/Ti ratios within a strong felsic composition, and do not point to an alkaline character (Fig. 8; Table 3).

Silurian strata is much homogeneous and close to a typical UCC composition with as well a mainly felsic dominance in the detrital

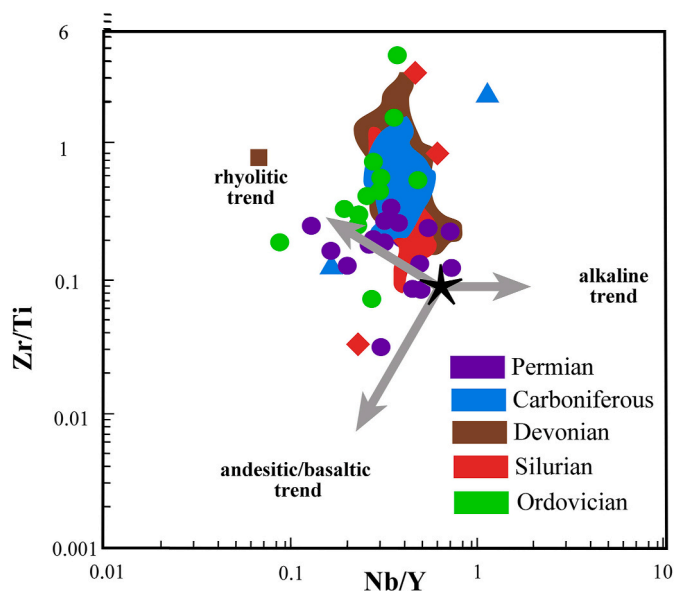


Fig. 8. General trace element composition based on Winchester and Floyd (1977). Shown are only the general trends and no discrimination fields. The star indicate typical UCC (according to McLennan et al., 2006). The black line indicates the outline of the brown field for Devonian rocks.

material.

Devonian rocks, including the Cumaná Formation, seem to be even stronger affected by felsic material with generally higher Zr/Ti ratios than the Silurian rocks, but comparable Nb/Y ratios.

The Carboniferous successions show a higher variety in Zr/Ti ratios but there is no trend towards a dominance of material other than felsic in the detrital mix. One sample of the Copacabana Formation has a very high Nb/Y ratio (Sample COPA13; Table 3) which is slightly depleted in Y and enriched in Nb.

Samples of the Chutani Formation show constantly lower Zr/Ti ratios than all others (Table 3; Fig. 8) in the stratigraphy but comparable Nb/Y ratio variations. This is the case for both, sandstones and marls and points to the emergence of a new source component.

Th/Sc versus Zr/Sc ratios (McLennan et al., 1990) are useful for clastic rocks because Zr/Sc ratios point to the degree of recycling with higher values (>30) pointing to significant sediment reworking, while the Th/Sc ratio would indicate the relation between felsic and mafic components in a clastic rock (Fig. 9).

The Ordovician formations, here studied, are variable but with high Zr/Sc values above 30 even up to 155 (Table 3; Fig. 9). Th/Sc ratios are as well far above 0,9 (value for typical UCC).

Within the Silurian successions the situation is slightly different. Samples from the Cancañiri Formation deposited at La Cumbre are nearly similar to typical UCC, while samples from the diamicite layers in the second exposure show partly strong recycled detritus with Zr/Sc ratios up to 346 (Table 3; Fig. 9). Rocks of the Uncía Formation show a similar character compared to the Cancañiri samples from La Cumbre, despite they are richer in silica. Samples from the Catavi Formation contain a stronger variation but tend to be dominated by felsic debris. Large variations in Zr/Sc ratios below 100 are caused by the lithotypes as several shales have been analysed, which often show lower Zr/Sc ratios (Taylor and McLennan, 1985; McLennan et al., 1990).

The Devonian rocks are generally recycled with Th/Sc and Zr/Sc ratios matching the Silurian deposits (Fig. 9). However, some samples are different. VV6 from the Vila-Vila Formation has low Th/Sc and Zr/Sc ratios, similarly, in the Belén Formation are three samples with comparable low ratios, from exposures 3 and 4 (3X1, 3X3 and 4X3; Table 3). In contrast, the stratigraphically following Devonian units are devoid of such samples and contain without exception highly recycled sandstones

(Table 3).

This changes significantly during the Carboniferous, when the Kasa Formation contains less samples with a recycled character and values comparable to typical UCC even in rocks with high silica content (e.g. KS9; Fig. 9; Table 3). Samples of the overlying Copacabana Formation have even lower Th/Sc and Zr/Sc ratios in average, which is caused by stronger variation in all three trace elements (Table 3; Fig. 9).

This trend can also be seen in the samples of the Chutani Formation, where several rocks show very low Th/Sc and Zr/Sc ratios, which is caused by Th depletion and not by enrichment in Sc (see Supplementary Table 1).

Often Rare Earth Elements (REE) are used to characterize rocks in terms of the origin or the detrital material (McLennan et al., 1990) and compiled in Table 4. However, mostly, sandstones and even shales show typical UCC patterns, which is the case in this study as well. Key values for the interpretation are (i) La/Yb_(N) ratios, which point to the steepness of the REE distribution with flatter pattern (lower La/Yb_(N) values) reflecting the dominance of less differentiated detritus within the detrital mix (McLennan et al., 1990), (ii) Ce* which can point to strong alteration (Wilde et al., 1996) and (iii) Eu* as a common indicator for the existence of the rather unstable plagioclase during reworking, within the remained sediment, where abundant plagioclase can reflect an intermediate or even mafic detrital component (McLennan et al., 1990).

Most of the samples of the Ordovician show total REE (Σ REE) comparable to UCC and Eu* anomalies typical for UCC (around 0,6) and Ce* values straddling 1, which does not point to either a strong reducing environment (far below 1) or strong oxidation (far above 1; Table 4). La/Yb_(N) ratios are also typical to UCC. The same can be observed for the Silurian Cancañiri Formation with only one sample depleted in Σ REE (CAN6; Table 4). This changes within the Uncía Formation with high Ce* values, mostly above 2, and very low Eu* values (<0,5) and steeper pattern even in silica-rich samples, hence not a consequence of the dilution effect of silica (Table 4). The same trend can be observed in the Catavi Formation, and both have mostly Σ REE comparable to typical UCC or carry even higher concentrations of REE (Table 4). Slightly flatter pattern with lower La/Yb_(N) than during the Silurian, are recorded in the Devonian with Ce* around 1 and Eu* between 0,4–0,7 (Table 4). More variation can be observed in the rocks of Carboniferous age. Especially Eu* increases in samples of the Kasa Formation often up to 0,8 and La/Yb_(N) varies strongly from 5,1 to 18,6. This cannot be stated for the rocks of the Copacabana Formation where REE values are typical for UCC (Table 4). The rocks of the Chutani Formation resemble the trend of the Kasa Formation with low Σ REE, variable Eu* and flat REE pattern (trend to low La/Yb_(N) ratios; Table 4).

2.3. Extraordinary observations

Besides the commonly used major and trace elements for the characterization of the rocks, we like to report significant extraordinary concentrations or trends within trace and minor elements. Riemann Reimann Zumsprekel et al. (2015) reported very high Cr concentration in Ordovician rocks. Similar high values from the other 162 samples are extremely rare and only six concentrations above 100 ppm were observed of which only two show significant enrichment (UN15 = 507 ppm and CH-38 = 198 ppm; Supplementary Table 2). Cr indicates in sediments the existence of chromite, a mineral pointing to the existence of a mafic source component and may occur even in strongly recycled rocks because it is relatively stable (Morton and Hallsworth, 1999). Besides the absolute concentration of Cr, ratios of Cr/V and Cr/Th would point to such an influence, when for the former ratio values above 10 trend to an 'ophiolitic' component (McLennan et al., 1993) and for the latter ratios above 40 to a significant ultramafic detrital factor (Floyd and Leveridge, 1987). Although higher chrome concentration have been observed in some post-Ordovician rocks, enrichments in V counters this enrichment out; this is, however, not the case for the Ordovician rocks. There are finally two post-Ordovician samples with elevated Cr

Table 3

Geochemical data of the Paleozoic successions with focus on typical values for provenance related interpretations. Please see for the complete data set [Supplementary Table 1](#). Color codes see [Table 1](#).

SAMPLES	Nb/Y	Zr/Ti	La/Sc	Ti/Zr	Th/Sc	Zr/Sc	SAMPLES	Nb/Y	Zr/Ti	La/Sc	Ti/Zr	Th/Sc	Zr/Sc
COROICO							SICA-SICA						
CORO 1	0.48	0.52	2.42	1.91	0.97	10.46	SS-1-a	0.33	1.19	7.25	0.84	2.37	106.87
CORO 10	0.26	0.07	3.99	14.00	1.18	30.30	SS-13-a	0.34	0.41	4.10	2.45	1.51	40.75
CORO 12	0.37	4.33	7.00	0.23	2.14	155.82	SS-14-a	0.37	0.64	4.79	1.56	1.86	65.94
CORO 14	0.20	0.32	7.98	3.11	1.63	81.93	SS13	0.37	0.41	3.89	2.42	1.48	39.28
CORO 16	0.25	0.41	5.55	2.44	1.35	79.83	SS14	0.34	0.74	6.00	1.36	2.40	80.80
CORO 17	0.29	0.70	6.56	1.43	2.00	116.98	SS4	0.30	0.82	5.43	1.22	2.63	92.23
AMUTARA							SS1						
AM 7	0.09	0.18	9.35	5.49	1.30	60.10	SS15	0.37	0.81	6.73	1.23	2.22	80.97
AM 9	0.35	1.49	7.22	0.67	2.38	142.80	SS19	0.38	0.70	5.67	1.43	2.13	62.97
AM 12	0.22	0.25	5.21	4.03	1.50	74.41	SS12	0.33	0.77	4.96	1.30	2.39	92.31
AM 15	0.31	0.42	5.12	2.36	1.50	71.83	SS2	0.34	0.53	5.41	1.87	1.86	50.31
AM 20	0.28	0.66	6.45	1.51	1.65	129.35	SS10	0.38	0.50	4.84	2.01	1.81	51.16
CANCANIRI							SS5						
CC44	0.44	0.12	2.99	8.19	0.87	6.27	SS11	0.42	0.37	4.36	2.73	1.49	36.62
CC49	0.41	0.18	3.11	5.57	1.02	12.03	COLLPACUCHO						
CC50	0.38	0.10	3.45	10.16	0.88	7.97	CLP-7b	0.40	0.62	5.93	1.62	1.97	74.09
CA2	0.47	0.16	3.38	6.19	0.94	10.82	CLP-5b	0.32	0.43	4.89	2.35	1.56	51.10
CA8	0.23	0.03	3.56	29.67	0.99	9.88	CLP-12 b	0.77	0.23	3.08	4.36	1.16	13.76
CA9	0.39	0.12	3.01	8.68	0.94	7.90	CLP2b	0.41	0.27	4.23	3.64	1.35	21.95
CA1	0.51	0.17	3.00	5.91	0.70	14.49	CLP13b	0.46	0.16	2.16	6.07	1.10	22.21
CA6	0.42	0.16	3.32	6.38	0.96	9.95	CLP9b	0.41	0.44	4.61	2.26	1.57	37.94
CA7	0.43	0.14	3.34	7.02	0.99	10.05	CLP1	0.41	0.32	3.75	3.11	1.15	25.67
CAN4	0.48	0.16	2.73	6.31	1.09	12.03	CLP12b	0.55	0.19	3.56	5.19	1.15	15.89
CAN5	0.48	0.35	2.98	2.89	1.11	23.70	CLP15	0.38	0.26	4.84	3.81	1.59	40.26
CAN8	0.47	0.17	2.59	5.97	1.05	13.01	CLP5	0.42	0.23	3.81	4.34	1.20	22.10
CAN9	0.49	0.20	2.61	4.96	1.09	12.77	CLP3b	0.37	0.45	4.62	2.24	1.55	40.07
CAN11	0.46	0.44	3.43	2.29	1.21	26.21	CLP7b	0.39	0.46	5.45	2.16	1.90	55.52
CAN12	0.47	0.39	4.32	2.57	1.26	28.72	CUMANÁ						
CAN13	0.44	0.50	4.21	2.01	1.32	41.78	CU1	0.34	1.23	5.49	0.81	1.86	55.25
CAN10	0.46	3.25	9.50	0.31	3.65	340.63	CU2	0.35	0.96	6.30	1.04	2.00	57.80
CAN6	0.47	0.52	3.12	1.92	1.32	56.08	CU4	0.36	0.56	4.57	1.79	1.66	37.29
CAN7	0.59	0.83	5.58	1.20	1.70	99.60	CU5	0.34	0.72	4.80	1.39	1.68	50.47
UNCIA							CU6-2						
UN1	0.46	0.22	2.93	4.54	0.93	16.27	CU6-3	0.34	0.74	5.53	1.29	2.97	46.60
UN2-A	0.43	0.12	3.27	8.00	0.97	14.48	CU6-4	0.34	0.40	6.24	2.52	1.60	28.56
UN2	0.47	0.32	2.73	3.13	1.06	19.18	CU6-5	0.31	1.14	6.10	0.88	2.13	68.40
UN3	0.46	0.15	2.82	6.78	0.96	12.71	CU7-1	0.33	1.16	5.58	0.87	2.00	60.63
UN4	0.50	0.16	3.06	6.11	0.94	12.69	CU7-2	0.29	1.36	6.66	0.74	2.72	81.30
UN6	0.51	0.23	2.81	4.36	1.06	13.76	CU8	0.29	0.32	6.10	3.11	1.63	32.17
UN7	0.47	0.24	2.83	4.20	1.02	23.80	CU9	0.36	0.80	5.69	1.26	1.63	35.76
UN8	0.48	0.21	2.85	4.80	0.94	13.28	KASA						
UN9	0.56	0.29	2.96	3.42	1.04	14.25	KAS-I-1	0.47	0.71	3.64	1.41	0.75	21.33
UN10	0.57	0.18	2.99	5.60	1.00	19.26	KAS-I-2	0.31	0.24	7.18	4.18	0.94	22.96
UN13	0.40	0.23	2.80	4.29	0.99	27.96	KS1	0.41	0.37	3.85	2.73	0.95	32.95
UN15	0.40	0.38	3.53	2.63	1.14	26.26	KS2	0.39	1.04	4.00	0.97	1.20	31.04
UN16	0.38	0.32	3.04	3.08	1.10	30.54	KS3	0.40	0.28	9.30	3.58	2.50	50.20
UN12	0.44	0.27	2.79	3.76	0.94	19.37	KS5	0.41	1.35	6.65	0.74	2.35	101.50
UN11	0.43	0.24	2.94	4.14	0.98	20.52	KS4	0.33	1.14	5.96	0.88	2.21	111.33
UN14	0.49	0.25	3.13	4.06	1.02	15.58	KS6	0.29	0.43	9.10	2.34	2.60	51.20
CATAVI							KS7						
CAT3	0.44	0.56	3.26	1.77	1.24	25.37	KS8	0.28	0.62	1.95	1.60	0.75	18.73
CAT4	0.33	0.86	7.25	1.17	2.65	89.93	KS9	0.30	0.93	4.35	1.08	1.25	27.75
CAT5	0.51	0.28	3.28	3.51	1.12	13.05	COPACABANA						
CAT6	0.41	0.52	3.45	1.93	1.21	26.25	COPA1a	0.26	0.55	4.41	1.81	0.99	24.81
CAT11	0.47	0.19	2.97	5.31	1.01	8.15	COPA2	0.55	0.51	2.05	1.97	1.30	38.03
CAT12	0.28	1.12	4.95	0.90	1.87	55.80	COPA3	0.27	0.67	7.61	1.50	1.13	49.99
CAT13	0.38	0.35	3.26	2.86	1.16	19.66	COPA4	0.50	0.46	2.18	2.20	1.13	34.11
CAT14	0.31	0.95	4.97	1.05	1.95	57.00	COPA6	0.29	0.74	7.26	1.36	1.09	55.15
CAT15	0.45	0.32	3.12	3.16	1.09	15.64	COPA7	0.17	0.13	5.73	7.53	0.69	13.94
CAT19	0.49	0.33	3.31	3.04	1.11	11.11	COPA8a	0.41	0.23	2.64	4.29	1.01	20.98
CAT20	0.32	0.49	2.66	2.05	1.01	23.80	COPA8b	0.44	0.24	2.51	4.20	0.90	20.84
CAT21	0.40	0.34	3.12	2.94	1.11	15.62	COPA10	0.28	0.60	7.34	1.66	1.03	41.19
CAT22	0.27	0.81	4.90	1.23	2.18	68.04	COPA11	0.43	0.50	8.84	2.02	1.07	46.19
CAT8	0.29	0.54	3.80	1.84	1.44	52.07	COPA13	1.14	2.28	2.81	0.44	3.10	17.09
CAT9	0.41	0.36	3.13	2.75	1.02	16.93	COPA14	0.43	0.30	2.36	3.29	0.86	19.74
CAT17	0.45	0.32	2.91	3.15	0.94	15.49	CUCO1	0.51	0.40	3.42	2.47	1.17	29.61
CAT18	0.30	0.38	3.29	2.65	1.15	32.08	GHUTANI						
VILA-VILA							Ch-2						
VV-1	0.33	0.59	6.16	1.68	1.86	64.18	Ch-4	0.38	0.27	1.10	3.75	0.20	16.00
VV-5	0.45	0.48	5.90	2.07	1.76	57.86	Ch-7	0.36	0.32	2.31	3.14	0.52	23.53
VV-12	0.34	1.31	11.87	0.76	4.30	209.83	Ch-8	0.40	0.24	2.21	4.24	0.67	22.63
VV7	0.32	0.59	5.80	1.69	2.08	71.10	Ch-11	0.42	0.24	1.61	4.19	0.41	12.41

(continued on next page)

Table 3 (continued)

SAMPLES	Nb/Y	Zr/Ti	La/Sc	Ti/Zr	Th/Sc	Zr/Sc	SAMPLES	Nb/Y	Zr/Ti	La/Sc	Ti/Zr	Th/Sc	Zr/Sc
VV6	0.33	0.51	6.85	1.96	2.23	76.63	Ch-12	0.16	0.16	2.13	6.17	0.55	11.66
VV2	0.32	0.56	5.70	1.78	1.76	60.78	Ch-13	0.32	0.18	2.33	5.45	0.62	14.68
VV13	0.24	1.02	10.67	0.98	3.63	163.73	Ch-16	0.29	0.03	1.83	32.09	0.58	14.17
VV15	0.40	0.40	4.77	2.49	1.60	44.10	Ch-18	0.30	0.18	2.06	5.44	0.50	11.03
VV16	0.54	0.16	2.61	6.34	0.89	8.93	Ch-20	0.47	0.13	1.80	7.76	0.83	23.16
VV11	0.23	1.20	11.57	0.84	3.80	191.30	Ch-21	0.44	0.09	1.75	11.57	0.75	22.28
VV8	0.42	0.44	5.38	2.30	1.66	52.18	Ch-22	0.49	0.09	1.77	11.58	0.75	22.27
BELEN							Ch-25	0.71	0.12	1.95	8.52	0.83	15.35
1 × 4GS	0.39	0.94	4.12	1.07	1.81	101.22	Ch-29	0.72	0.22	2.53	4.46	0.32	17.92
1 × 1GS	0.35	1.99	4.26	0.50	1.96	95.54	Ch-30	0.46	0.17	1.83	5.91	0.37	13.52
1 × 2GS	0.41	2.86	5.24	0.35	2.28	171.56	Ch-32	0.53	0.24	2.89	4.25	0.25	12.92
1 × 3GS	0.41	1.59	4.39	0.63	1.61	81.57	Ch-35	0.74	0.22	2.29	4.55	0.27	13.16
2 × 2GS	0.46	0.57	3.13	1.77	1.14	31.33	Ch-36	0.28	0.20	1.66	4.95	1.02	12.10
2 × 4GS	0.37	0.83	3.39	1.20	1.48	56.23	Ch-38	0.32	0.27	2.18	3.71	0.27	8.08
2 × 1GS	0.46	0.54	3.03	1.84	1.12	25.05	Ch-39	0.13	0.26	1.73	3.82	1.02	13.08
2 × 3GS	0.28	0.19	3.54	5.20	1.46	53.06							
3 × 4GS	0.36	1.63	5.20	0.61	2.13	97.65							
3 × 1GS	0.50	0.87	3.21	1.15	0.91	20.03							
3 × 2GS	0.40	1.44	3.78	0.70	1.70	86.18							
3 × 3GS	0.49	0.88	2.74	1.14	0.87	26.35							
4 × 1GS	0.42	0.68	4.08	1.47	1.49	50.83							
4 × 2GS	0.53	0.37	2.93	2.71	1.15	25.80							
4 × 4GS	0.39	0.77	3.51	1.30	1.17	18.50							
4 × 3GS	0.49	0.62	2.92	1.62	1.02	25.63							

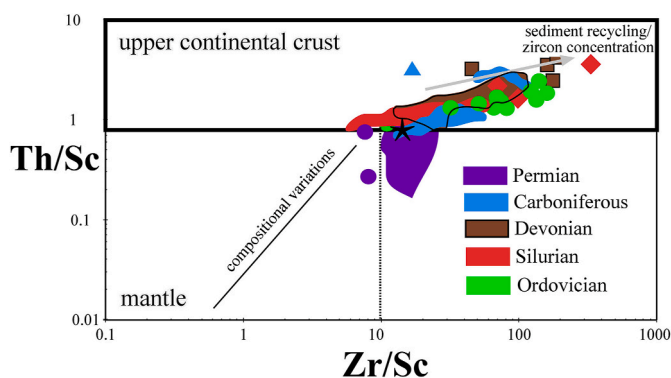


Fig. 9. Recycling of sediment detritus versus the differentiation of the mix is portrayed by Th/Sc versus Zr/Sc ratios (after McLennan et al., 1990). The star indicate typical UCC.

concentrations: UN15 with 507 ppm and CH-38 with 197 ppm. All other samples do not show any significant enrichment of a trace element (Supplementary Table 2).

Total sulfur is nearly absent in the entire post-Silurian stratigraphy, total carbon with values higher than 0,7% exist only in three samples of the Catavi Formation. Although the shales of the Cancañiri Formation are dark blue even black, their total organic concentrations of C are below the detection limit and do not rise above 0,22 wt% (Supplementary Table 1).

Within the entire stratigraphy are only very few samples enriched in base metals, Cr in Ordovician rocks has been mentioned above. V is enriched in Silurian rocks compared to all other formations but only with two samples with relatively high values above 200 ppm. Zn is in some samples of Ordovician and Silurian rocks enriched compared to typical UCC. The same is the case for Bi, Sb, Se, Sn and W although the region is world famous for base metal mining. Moreover, some of the base metals are redox-sensitive and therefore enrichment may be related to the depositional environment and not to a mafic provenance (see below; Supplementary Table 1; see also Lehmann et al., 2000).

3. Discussion

Paleogeographic studies determined in regard of the basin evolution,

a steady depositional center, which had been sandwiched between a major eastern source, the Sunsas belt and a major western source, represented by the Arequipa Massif, for the here discussed study area (França et al., 1995; Reimann Zumsprekel et al., 2015). Very few is known about sediment transport directions as paleocurrent indicators are not reported. Reimann Zumsprekel et al. (2015) reports Bouma sequences in the Ordovician rocks, and a still deep marine environment but with a clear dominance of shales, maybe a fjord-type environment during the deposition of the Cancañiri Formation with a subsequent constant shallowing during the Silurian. Possibly deltaic but definitely shallow marine platform deposits partially with the deposition of turbidity currents characterize the Devonian with possible intercalation of glacial (Díaz Martínez and Isaacson, 1994) (or not) diamictites within the Cumaná Formation. Maybe parts of the Kasa Formation have been deposited on land but the deposits of the overlying Carboniferous successions are again shallow marine. The Permo-Triassic Chutani Formation is definitely marine at its base, but may record, similar to the Kasa Formation, continental deposits based on identified land plants (Iannuzzi et al., 2004; Vieira et al., 2004). This indicates mostly a shallow marine, coastal, depositional environment for all post-Cancañiri successions.

Petrographically changes are as well rather minor throughout the stratigraphy with two exceptions. The Ordovician displays strongly reworked sandstones which have been classified as quartz-arenites composed of well-rounded and moderately to good sorted clasts (Reimann Zumsprekel et al., 2015). This is unique within the entire Paleozoic on a formation level. All other formations are characterized by rather subangular to subrounded clastic material. This accounts also for the source of detrital zircons as described by Iriarte et al. (2021). While Silurian and Devonian rocks and the Lower Carboniferous Kasa Formation are moderately sorted, a larger variation of grain sizes begins with the Copacabana Formation (Fig. 6). Within the Copacabana Formation pyroclastites have been reported (Hamilton et al., 2016) and volcanic rocks are described for the Triassic Tiquina Formation, overlying the Chutani deposits. In the Chutani Formation volcanoclastic arenites which contain quartz clasts with resorption embayments pointing to a volcanic source and possible epiclastic layers have been identified. We observe more abundant plagioclase in the rocks of the Chutani Formation (Fig. 6c–e) but no mafic volcanic lithoclasts which may indicate that (mafic) volcanic activity was still distal to the depositional area. Possibly the heavy mineral record would give more information about the influence of a mafic (volcanic) source.

Table 4

Geochemical data of the Paleozoic successions with focus on the rare earth element composition. Please see for the complete data set [Supplementary Table 1](#) and calculation of Ce* and Eu* the chapter methodology. La/Yb are chondrite normalized values. Green indicate Ordovician rocks, red Silurian samples, brown Devonian ones, blue those from Carboniferous successions and violet Permian strata. Color codes see [Table 1](#). Σ REE = sum of rare earth elements.

SAMPLES	SREE	Ce*	Eu*	La/Yb	SAMPLES	SREE	Ce*	Eu*	La/Yb	SAMPLES	SREE	Ce*	Eu*	La/Yb
COROICO					VILA VILA					KASA				
CORO 1	211.36	0.94	0.57	8.30	VV-1	149.98	0.97	0.50	8.46	KAS-I-1	123.3	0.81	0.92	10.14
CORO 10	296.68	0.97	0.64	7.51	VV-5	143.47	0.97	0.58	8.37	KAS-I-2	145.29	0.71	1.40	11.50
CORO 12	174.61	1.03	0.44	9.38	VV-12	185.92	1.06	0.46	7.20	KS1	45.99	1.24	0.94	5.10
CORO 14	176.53	1.10	0.58	8.91	VV7	145.6	0.99	0.52	7.81	KS2	150.16	0.86	0.62	8.48
CORO 16	123.76	1.02	0.55	8.02	VV6	136.81	1.00	0.56	8.38	KS3	42.3	0.98	0.80	8.49
CORO 17	172.57	1.04	0.53	7.80	VV2	140.51	0.98	0.54	8.09	KS5	130.24	0.99	0.51	8.64
AMUTARA					VV13	162.32	1.02	0.44	7.59	KS4	236.38	0.95	0.49	7.43
AM 7	102.37	1.06	0.58	9.09	VV15	141.18	0.97	0.59	8.48	KS6	42.8	0.93	0.81	8.54
AM 9	180.48	1.02	0.51	7.41	VV16	221.08	0.92	0.61	9.57	KS7	47.26	1.01	0.70	11.11
AM 12	207.49	0.99	0.53	7.01	VV11	179.49	1.01	0.47	7.64	KS8	42.78	1.02	0.81	5.38
AM 15	163.66	1.02	0.56	7.77	VV8	132.67	0.98	0.59	7.97	KS9	40.89	0.98	0.85	7.54
AM 20	132.98	1.05	0.53	7.23	BELEN					COPACABANA				
CANCANIRI					1 × 4GS	199.77	0.92	0.50	5.61	COPA1a	177.54	0.90	0.73	10.28
CC44	315.81	0.98	0.59	9.43	1 × 1GS	112.39	1.01	0.39	5.31	COPA2	84.59	0.91	0.69	4.64
CC49	264.35	0.99	0.64	10.13	1 × 2GS	132.2	0.97	0.44	5.79	COPA3	283.69	0.94	0.55	9.50
CC50	351.80	1.00	0.62	9.26	1 × 3GS	147.96	0.95	0.47	6.69	COPA4	83.42	0.85	0.64	5.16
CA2	303.22	1.01	0.61	10.71	2 × 2GS	205.48	0.97	0.55	6.58	COPA6	284.21	0.99	0.57	8.80
CA8	358.10	0.95	0.60	8.32	2 × 4GS	138.36	0.95	0.52	5.67	COPA7	245.2	1.01	0.60	11.34
CA9	319.28	0.98	0.61	8.62	2 × 1GS	195.93	0.93	0.55	6.41	COPA8a	143.54	0.86	0.57	6.89
CA1	192.06	0.96	0.62	10.24	2 × 3GS	89.98	0.82	0.82	4.82	COPA8b	147.43	0.87	0.54	6.42
CA6	267.14	0.94	0.61	10.86	3 × 4GS	151.89	0.92	0.50	6.67	COPA10	238.25	0.89	0.59	12.68
CA7	270.63	0.96	0.63	10.58	3 × 1GS	204.18	0.96	0.57	6.94	COPA11	382.33	1.01	0.51	18.61
CAN4	211.65	0.98	0.64	8.58	3 × 2GS	115.8	0.94	0.54	5.27	COPA13	111.28	1.05	0.61	7.10
CAN5	201.86	0.96	0.60	7.57	3 × 3GS	187.55	0.96	0.52	6.86	COPA14	114.69	0.79	0.56	6.64
CAN8	243.9	1.16	0.60	8.15	4 × 1GS	163.2	1.00	0.50	6.38	CUCO1	135.56	0.88	0.72	10.10
CAN9	262.04	1.07	0.58	7.49	4 × 2GS	167.72	0.95	0.50	7.00	CHUTANI				
CAN11	234.47	0.94	0.67	7.60	4 × 4GS	257.85	0.94	0.55	7.74	Ch-2	22.43	1.38	0.60	3.60
CAN12	281.99	0.99	0.63	9.19	4 × 3GS	189.07	0.96	0.53	7.09	Ch-4	6.05	1.19	0.81	7.43
CAN13	207.48	1.00	0.58	9.36	SICA SICA					Ch-7	139.67	0.82	0.66	8.55
CAN10	179.14	0.94	0.59	6.62	SS-1-a	207.88	0.95	0.42	7.73	Ch-8	101.95	0.79	0.63	7.32
CAN6	83.36	1.05	0.58	5.12	SS-13-a	247.34	0.97	0.52	6.61	Ch-11	114.16	0.88	0.78	8.98
CAN7	106.55	0.91	0.56	10.25	SS-14-a	160.31	0.96	0.52	6.36	Ch-12	111.13	0.89	0.82	6.60
UNCIA					SS13	238.64	0.96	0.54	6.34	Ch-13	129.83	0.85	0.78	8.34
UN1	193.7	2.10	0.28	10.70	SS14	170.74	0.94	0.43	6.63	Ch-16	131.17	0.99	0.75	6.11
UN2-A	237.73	2.19	0.22	13.56	SS4	210.75	0.95	0.46	5.48	Ch-18	97.8	0.91	0.78	7.95
UN2	113.67	2.12	0.30	11.60	SS1	192.51	0.94	0.51	7.66	Ch-20	73.58	0.84	0.61	5.20
UN3	223.12	2.03	0.30	12.67	SS15	190.19	0.92	0.47	8.58	Ch-21	95.13	0.90	0.60	4.91
UN4	252.94	2.12	0.26	14.47	SS19	163.25	0.97	0.50	7.81	Ch-22	94.11	0.86	0.61	4.92
UN6	239.3	2.13	0.27	12.45	SS12	196.99	0.96	0.54	5.81	Ch-25	104.13	0.80	0.67	7.23
UN7	129.01	2.23	0.28	10.32	SS2	180.32	0.96	0.51	7.32	Ch-29	63.63	0.77	0.54	14.07
UN8	219.3	2.02	0.28	12.13	SS10	161.52	0.96	0.52	7.18	Ch-30	75.74	0.76	0.60	10.42
UN9	236.55	2.08	0.25	11.85	SS5	173.76	0.93	0.50	6.44	Ch-32	154.72	1.00	0.65	12.41
UN10	166.67	2.21	0.27	11.16	SS11	182.61	0.93	0.53	7.77	Ch-35	141.36	0.99	0.65	16.02
UN13	106.8	1.94	0.31	10.16	COLLPACUCHO					Ch-36	46.99	0.88	0.65	2.18
UN15	223.56	2.14	0.28	12.41	CLP-7b	209.51	0.94	0.53	7.66	Ch-38	55.83	0.81	0.66	6.86
UN16	110.2	2.14	0.27	7.92	CLP-5b	199.17	0.99	0.56	7.30	Ch-39	63.28	0.87	0.67	1.74
UN12	196.28	2.15	0.29	11.44	CLP-12 b	156.2	1.04	0.57	11.25					
UN11	177.41	2.09	0.30	11.28	CLP2b	127.01	1.01	0.52	8.89					
UN14	273.51	2.07	0.25	12.88	CLP13b	85.08	0.94	0.64	6.12					
CATAVI					CLP9b	163.44	1.00	0.56	8.53					
CAT3	320.06	2.05	0.26	12.50	CLP1	113.22	1.00	0.53	8.35					
CAT4	140.98	2.10	0.20	10.62	CLP12b	146.93	1.03	0.54	10.64					
CAT5	265.34	2.05	0.26	12.63	CLP15	214.26	0.97	0.56	7.94					
CAT6	230.6	2.18	0.28	10.82	CLP5	193.6	1.01	0.57	8.47					
CAT11	267.47	1.93	0.27	14.15	CLP3b	137.6	1.00	0.51	8.32					
CAT12	152.79	2.17	0.18	8.46	CLP7b	165.9	0.95	0.56	8.53					
CAT13	252.04	2.09	0.27	11.11	CUMANÁ									
CAT14	149.61	2.12	0.20	10.92	CU1	222.99	0.96	0.52	7.16					
CAT15	262.76	2.05	0.25	12.70	CU2	185.78	0.94	0.58	7.74					
CAT19	248.88	2.03	0.25	13.98	CU4	198.5	0.92	0.55	7.82					
CAT20	227.56	2.20	0.29	8.40	CU5	146.76	0.97	0.55	7.29					
CAT21	263.16	2.11	0.28	11.77	CU6-2	111.55	0.96	0.53	2.31					
CAT22	133.27	2.24	0.20	9.07	CU6-3	134.51	0.95	0.62	10.29					
CAT8	196.73	2.12	0.31	8.21	CU6-4	150.55	0.94	0.56	11.78					
CAT9	269.14	2.05	0.25	12.10	CU6-5	120.74	0.95	0.51	7.46					
CAT17	224.88	2.10	0.25	12.10	CU7-1	220.96	0.93	0.49	6.85					
CAT18	205.93	2.17	0.27	9.73	CU7-2	175	0.95	0.55	7.58					
					CU8	91.38	0.95	0.65	9.09					
					CU9	233.93	0.98	0.50	8.03					

Caption muss: La/Yb normalized; SREE in ppm.

Table 5

Averages of the geochemical data of the Paleozoic successions per formation. Please see for the complete data set [Supplementary Table 1](#). Color codes see [Table 1](#). PPM = parts per million; % = weight percent. LOI = loss on ignition; ΣREE = sum of rare earth elements. 'N' = indicates normalized to chondrite after [Taylor and McLennan \(1985\)](#).

SAMPLES	CIA	K/Cs	Th/U	U/Th	SiO ₂	Al ₂ O ₃	Fe ₂ O _{3t}	MgO	CaO	Na ₂ O	K ₂ O	TiO ₂	P ₂ O ₅	MnO	LOI	sum	TOT/C	TOT/S	Ba	Rb	Sr	Cs	Cr	V	Ni
	%	%	%	%	%	%	%	%	%	%	%	%	%	%	%	%	%	%	PPM	PPM	PPM	PPM	PPM	PPM	PPM
COROICO	77	12,368	4.80	0.21	82.0	8.5	3.9	0.8	0.3	0.4	1.5	0.6	0.2	0.0	2.0	100.3			270	65.5	57.6	3.5	279.8	51.7	110.9
AMUTARA	61	5877	4.68	0.22	88.3	4.5	3.0	0.7	0.7	0.7	0.7	0.5	0.2	0.0	0.8	100.1			145	32.4	97.1	2.4	568.6	22.2	264.9
CANCANIRI	76	4281	4.72	0.22	66.1	17.0	6.2	1.5	0.3	0.6	3.4	0.9	0.2	0.1	3.5	99.8	0.19	0.08	639	140.4	100.9	7.1	73.9	101.5	26.3
UNCIA	78	2239	4.72	0.21	68.7	14.5	7.1	1.4	0.3	0.6	2.4	0.8	0.2	0.0	3.8	99.8	0.33	0.11	327	113.0	47.9	9.9	88.7	93.1	30.6
CATAVI	74	1287	4.46	0.23	69.0	15.1	4.9	1.1	0.2	0.8	3.2	0.8	0.1	0.0	4.5	99.8	0.49	0.13	381	166.0	31.8	22.1	62.2	93.7	20.8
VILA-VILA	69	7942	4.91	0.20	81.5	7.7	2.6	1.2	0.4	0.2	2.1	0.4	0.1	0.0	3.6	99.9	0.40	0.04	279	72.4	83.8	2.9	28.8	39.1	10.0
BELEN	73	4451	4.44	0.23	77.6	10.5	3.9	0.1	0.6	0.3	2.1	0.7	0.1	0.0	3.4	99.3	0.05	0.00	272	91.4	68.8	4.8	40.8	76.8	13.2
SICA-SICA	68	4774	4.12	0.24	76.7	10.6	4.7	0.9	0.2	1.8	1.4	0.7	0.1	0.0	2.6	99.9	0.11	0.00	231	63.9	73.0	2.6	54.9	56.5	20.5
COLLPACUCHO	67	5874	5.19	0.20	75.8	10.6	5.5	0.9	0.3	2.0	1.3	0.5	0.1	0.0	2.9	99.9	0.21	0.01	241	54.0	74.5	1.9	48.7	62.7	15.0
CUMANÁ	61	9110	4.59	0.22	79.6	10.0	2.2	0.5	0.2	1.7	3.0	0.5	0.1	0.0	2.4	99.9	0.12	0.00	417	75.9	85.5	2.8	38.9	38.9	9.6
KASA	60	18,992	4.32	0.28	83.9	8.2	1.3	0.4	0.2	2.1	1.7	0.2	0.0	0.0	1.9	100.0	0.09	0.00	207	40.1	52.1	0.9	23.7	29.5	4.9
COPACABANA	64	5604	3.33	0.33	58.0	12.8	3.5	2.1	7.6	1.0	4.2	0.6	0.1	0.1	9.9	99.9	1.71	0.01	341	117.0	67.5	6.7	19.3	61.3	6.6
CHUTANI	31	29,932	3.30	1.01	60.5	9.6	3.4	1.7	9.2	3.0	2.7	0.5	0.2	0.1	9.1	99.9	1.98	0.00	313	58.8	266.5	1.1	31.8	89.6	7.4
	Nb	Ta	Y	Zr	Hf	Sc	Th	U	Pb	Ga	Zn	Mo	La	Ce	Pr	Nd	Sm	Eu	Gd	Tb	Dy	Ho	Er	Tm	Yb
	PPM	PPM	PPM	PPM	PPM	PPM	PPM	PPM	PPM	PPM	PPM	PPM	PPM	PPM	PPM	PPM	PPM	PPM	PPM	PPM	PPM	PPM	PPM	PPM	PPM
COROICO	10.8	0.8	35.0	432	11.8	8.2	10.9	2.2	7.0	11.3	39.0		36.2	79.6	9.4	36.4	7.8	1.5	6.6	1.1	5.8	1.1	3.1	0.5	3.0
AMUTARA	7.9	0.7	30.6	461	12.7	4.8	8.1	1.8	4.2	5.3	20.0		29.6	65.5	7.6	28.4	6.2	1.2	5.7	1.0	5.0	1.0	2.7	0.4	2.7
CANCANIRI	15.9	1.1	37.3	301	8.6	14.5	15.4	3.3	32.5	20.2	98.5	0.3	48.4	102.7	11.7	45.0	8.8	1.8	8.1	1.2	7.1	1.4	3.9	0.6	3.7
UNCIA	14.7	1.2	31.3	227	6.5	13.0	13.0	2.8	16.4	16.8	81.6	0.8	38.7	79.6	9.3	35.9	7.0	1.4	6.4	1.0	5.7	1.1	3.4	0.5	3.3
CATAVI	15.1	1.2	38.6	321	9.5	13.4	16.1	3.6	12.5	16.4	76.4	0.3	45.1	91.8	10.7	41.4	7.8	1.5	7.4	1.2	6.8	1.4	4.0	0.6	4.0
VILA-VILA	8.6	0.8	24.2	360	9.5	5.6	10.5	2.1	5.2	7.9	28.9	0.1	31.8	66.8	7.4	28.2	5.5	1.0	5.1	0.8	4.4	0.9	2.7	0.4	2.6
BELEN	13.1	1.1	30.9	464	12.2	9.6	12.7	2.9	7.2	13.1	34.3	0.4	33.5	67.6	7.8	29.4	5.8	1.0	5.5	0.9	5.5	1.1	3.4	0.5	3.6
SICA-SICA	12.3	1.0	34.8	480	12.8	7.9	15.0	3.7	18.4	10.7	64.9	0.3	39.6	79.3	8.9	33.2	6.1	1.0	5.7	1.0	6.0	1.3	4.0	0.6	3.9
COLLPACUCHO	9.4	0.7	22.2	256	6.8	7.6	10.7	2.1	13.6	11.4	45.8	0.2	31.6	67.4	7.7	29.6	5.6	1.0	4.7	0.7	4.2	0.9	2.6	0.4	2.6
CUMANÁ	9.2	0.8	33.2	286	7.9	5.8	11.1	2.5	11.1	8.6	40.7	0.4	32.7	66.8	8.0	30.3	5.8	1.1	5.9	1.0	6.0	1.2	3.4	0.5	3.1
KASA	5.2	0.4	14.4	200	5.3	4.0	5.7	1.4	5.5	8.0	9.6	0.3	20.3	38.9	4.7	17.4	3.1	0.8	2.7	0.4	2.6	0.5	1.6	0.2	1.6
COPACABANA	10.8	0.7	27.1	277	7.2	9.1	10.5	3.4	19.9	13.4	14.5	1.5	39.3	78.0	9.0	34.0	6.3	1.2	5.7	0.9	4.9	1.0	3.0	0.4	2.9
CHUTANI	6.7	0.4	17.8	144	3.6	9.1	5.1	5.0	9.5	8.7	43.1	1.6	18.7	35.4	4.3	17.1	3.3	0.8	3.1	0.5	3.0	0.6	1.9	0.3	1.9
	Ce*	Eu*	La/YbN	Nb/Y	Zr/Ti	La/Sc	Ti/Zr	Zr/Sc	Th/Sc	Sc/Th	Cr/Th	Cr/V	Y/Ni												
COROICO	1.02	0.55	8.32	0.31	1.06	5.58	3.85	79.22	1.55	0.70	40.27	10.46	0.62												
AMUTARA	1.03	0.54	7.70	0.25	0.60	6.67	2.81	95.70	1.67	0.63	67.56	26.07	0.46												
CANCANIRI	0.99	0.61	8.85	0.45	0.42	3.70	6.22	39.15	1.22	0.92	4.79	0.78	1.62												
UNCIA	2.11	0.28	11.69	0.47	0.24	2.97	4.56	18.74	1.01	1.00	6.43	0.94	1.07												
CATAVI	2.10	0.25	11.13	0.38	0.51	3.74	2.43	32.12	1.37	0.80	3.69	0.70	3.74												
VILA-VILA	0.99	0.53	8.14	0.36	0.66	7.02	2.08	90.97	2.32	0.52	2.76	0.92	3.85												
BELEN	0.95	0.53	6.30	0.42	1.05	3.72	1.45	60.41	1.46	0.75	3.22	0.57	9.14												
SICA-SICA	0.95	0.50	6.98	0.36	0.64	5.23	1.72	64.39	1.97	0.53	3.74	0.98	1.73												
COLLPACUCHO	0.99	0.55	8.50	0.44	0.34	4.24	3.43	35.05	1.44	0.72	4.55	0.78	1.53												
CUMANÁ	0.95	0.55	7.78	0.31	0.85	5.71	1.42	49.14	1.96	0.53	3.44	0.97	4.01												
KASA	0.95	0.81	8.39	0.35	0.70	5.97	1.92	49.57	1.67	0.77	6.22	1.11	6.95												
COPACABANA	0.92	0.61	9.09	0.44	0.59	4.55	2.67	31.67	1.19	0.95	2.02	0.40	9.06												
CHUTANI	0.91	0.68	7.54	0.41	0.19	1.98	7.17	15.38	0.57	2.19	12.91	0.53	2.93												

A definite volcanic component is absent in all other formations (pre-Copacabana) and we observe during the late Paleozoic a shorter sediment transport than before. This may be caused by a narrowing of the basin, quicker sedimentation rates and/or by reduction of the accommodation space and shorter intra-basinal transport (França et al., 1995). However, most important is the fact that detritus from metamorphic basement rocks (gneisses, schists, polycrystalline quartz grains, etc.) is nearly absent within the entire stratigraphy.

Geochemical changes are as well rather difficult to pin point because not very strong. CIA and alteration vary throughout the stratigraphy and show a trend from stronger weathered to less strong (Fig. 7). An exception are the rocks of the Amutara Formation and here the low CIA may be related to the dilution effects by extreme high silica values (Supplementary Table 1 and Table 5). Rocks of the Cumaná Formation are interpreted as related to a glacial environment, and so possibly the base of the Kasa Formation, which could explain here lower values (Table 5; Supplementary Table 1). CIA values for the Copacabana and Chutani Formation are mostly difficult to interpret because of the partly high CaO concentrations. However, K/Cs ratios assist here and show a similar trend from the Ordovician to the Collpacucho deposits with moderate to strong weathering and values lower than typical UCC or even lower than those for shales (Table 5; Supplementary Table 1; Fig. 7). Higher K/Cs values appear systematically from the diamictite deposits of the Cumaná Formation stratigraphically up (Table 5). The lower values of CIA and higher ratios of K/Cs may support the suggestions that transport of the detritus was shorter and affected both values (CIA and K/Cs) after the erosion from the source areas. Such a trend could also be caused by higher sedimentation rates with more rapid burial of the detritus and less pronounced reworking within the depositional area, as the petrography (see above) suggests. Additionally, Th/U ratios which may be able to indicate stronger weathering with higher values, because U is lost during recycling under oxygenated environments (McLennan et al., 1990, 1993), does not change over time, besides lower values for the late Paleozoic formations (Table 5; Supplementary Table 1).

The general composition based on REE, Nb/Y, Zr/Sc, Th/Sc and Zr/Ti ratios did not vary strongly through time and reflect definitely a constant dominance of felsic detritus (Tables 2 and 3; Figs. 8 and 9). Nb/Y ratios could not identify any changes in the overall alkalinity of the sediment mix and Zr/Ti ratios are for nearly all formations high and reflect a rhyolitic composition (after Winchester and Floyd, 1977, Fig. 8). Using Th/Sc and Zr/Sc ratios a similar trend is observed (Fig. 9): no strong changes throughout the stratigraphy with one exception: Chutani Formation. In the latter, Th/Sc and Zr/Sc ratios vary strongly and several samples point to the existence of a new source component, but mainly driven by slightly lower concentrations of incompatible elements than an increase of compatible ones. Nb, Ta and Ti even decrease and this could be, together with the few remnants of volcanic activity, point to the influence of a volcanic arc source (Hofmann, 1988, 1997). However, this is an interpretation and needs more substantiation by dating of detrital material and studies of the heavy mineral suites within the formation and the overlying Tiquina Formation. Nevertheless, the overall compositional maturity of the rocks is slightly lower, as mentioned above, a trend which started during the deposition of the Copacabana Formation.

To identify a paleotectonic setting within clastic rocks several diagrams have been proposed (Bhatia and Crook, 1986; McLennan et al., 1990, 1993; besides others). The plots are using the same trace elements (La, Sc, Zr, Ti) and they obviously do not identify the paleotectonic setting of the succession but the character of the clastic mix and they are here applied (Fig. 10). In some cases, when synsedimentary lavas are studied and contribute also significantly to the detrital material then these diagrams may be able to allow interpretation of SYN-sedimentary paleotectonic settings as it was possible in the here discussed region in the Ordovician arc deposits of northern Chile (e.g. Zimmermann et al., 2010), southern Peru (Bahlburg et al., 2006) and northwest Argentina

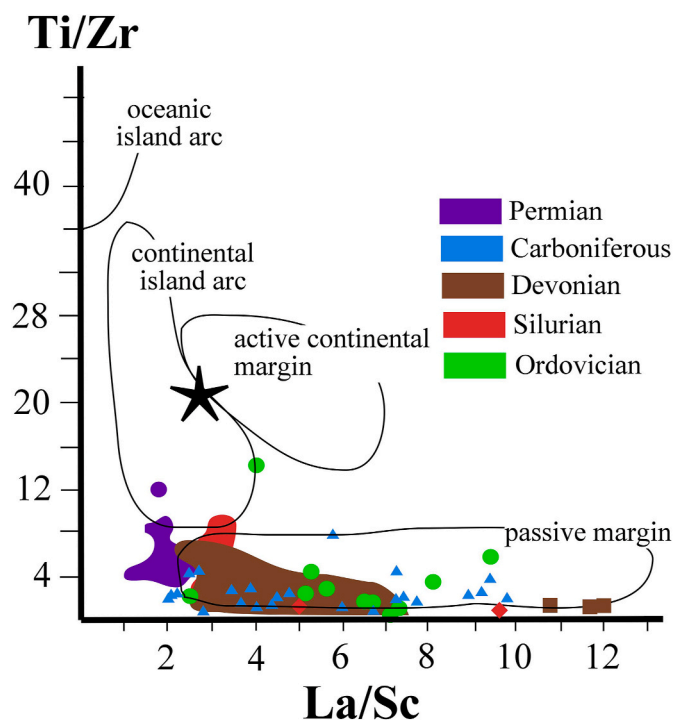


Fig. 10. La/Sc versus Ti/Zr try to determine the general paleotectonic fingerprint of sedimentary mixes (known that the ages of the detritus is differs strongly; after Floyd et al., 1990). General defined fields are in weakly displayed and the trends, which are reflecting the main source component are marked by dark black arrows.

(e.g. Bahlburg, 1990, 1998; Zimmermann et al., 2003). Here, this is not the case. La/Sc ratios needs to be rather low (<3) and Ti/Zr ratios high (>20) to recognize the dominance of a non-felsic component in the detrital mix (Fig. 10; Table 5). These criteria can only two samples fulfill (CA-6 and CH-16). This does not exclude mafic input into the detritus but assigns a clear dominance of felsic detrital material throughout the entire stratigraphy. Some samples are slightly stronger recycled and within the Carboniferous formations a wide spread of La/Sc is observable which can be explained by poor mixing of stronger recycled and less reworked detritus. Rocks of the Chutani Formation have the lowest La/Sc and Th/Sc ratios (Figs. 9 and 10; Table 5 which is not a result of enrichment of Sc in regard of typical UCC, but a depletion of incompatible elements like La and Th. This, combined with depletion in Nb, Ta and TiO₂ (besides in two samples; CH-7 with 0,83 wt% TiO₂ and CH-29 with 14,3 ppm Nb; Supplementary Table 1), may be a hint for the emergence of a continental arc and its detrital influence (Hofmann, 1988, 1997), but needs definitely more detailed studies using heavy minerals. Pyroclastic layers are reported and we found definitely higher amounts of clays and illite within the petrography (Fig. 6d and f), but we are not able here to report the geochemical composition of those fine layers.

Mafic or even intermediate input can be monitored either by absolute concentrations of compatible elements like (Nb, Ta, Cr, V, Ni, Ti, Cu, Sc, or Co) or specific ratios (Sc/Th, Cr/Th, Cr/V, Y/Ni; Floyd et al., 1990; McLennan et al., 1990, 1993). Some of these elements are, however, redox-sensitive (Cr, V, Ni, Cu; Calvert and Pedersen, 1993; see below). Table 5 (or the Supplementary Table 1) and none of the shown figures 7–10 shows any significant change or input of an even intermediate source component, within the detrital mixes, often the material does not match typical UCC. This implies a significant dominance of felsic detritus during the entire stratigraphy. Regarding the mentioned possible occurrence of significant compatible elements in the detritus, only Ordovician samples show a strong increase in two base metals: Cr and Ni. However, Reimann Zumsprekel et al. (2015) could not find the

bearer of this provenance signal and argued that this may be an artefact of sorting, as they studied the fraction coarser than 63 μm .

An-oxic conditions can be traced by the enrichment of redox sensitive base metals like Mn, Cr, Cd, Cu, Ni, U, V and Zn (Calvert and Pedersen, 1993), U/Th ratios above 0.75 (Jones and Manning, 1994) and Ce* values significantly below 0 (Wilde et al., 1996; Pattan et al., 2005) of which, as discussed, some are candidates to point to a different source component. Within the Chutani Formation few changes are observable like introduction of V, Mo and Cu and a depletion in some incompatible elements like Th, La and Zr (Table 5). Molybdenum enrichment is reported during early diagenetic take-up by carbonate phases (Romaniello et al., 2016; Midgley et al., 2020) and could explain the higher values for Mo here. All other mentioned elements values are not enriched or pointing to an-oxic conditions within the Chutani Formation (Supplementary Table 1). This coincides with the facies observation, which argues for a very shallow marine if even not continental depositional environment (Iannuzzi et al., 2004; Vieira et al., 2004). Molybdenum enrichment is often observed related to glacial diamictites (e.g. Young et al., 2000) because of their trend to be less exposed to oxic conditions. This cannot be stated for the samples, here collected, from the Cancañiri or the Cumaná formations (Table 5; Supplementary Table 1). In summary, U/Th ratios, Ce* and normalized values for Mn, Cr, Ni, Zn, Mo, V and Cu (according to Calvert and Pedersen, 1993, Table 5; Supplementary Table 1) do not point to a significant an-oxic environment for any of the studied successions as only in very few formations some samples show enriched values (Supplementary Table 1). This implies that the enrichment of Cr and V in the two Ordovician successions has a detrital origin.

Petrographic and geochemical data from the studied Paleozoic samples in northwestern Bolivia do not reflect paleotectonic changes because the detrital signal for those changes, observed to the north and south of the study area, never arrived in the depositional center here studied. Reworking within the stratigraphy did not take place, as the sediments do not increase in their compositional or textural maturity (Figs. 3–6 and geochemical plots in Figs. 7–10) and we could not find any sedimentary lithoclast of older formations reworked into the younger ones. Based on the nearly entire lack of metamorphic detritus, it is not explainable that the mentioned orogenic belts, Arequipa Massif and the Sunasas belt with their known lithological composition of mainly low grade to high grade metamorphic rocks are the direct proto-sources. Recycling from those areas should have produced more metamorphic detritus or rounded and reworked silica-rich samples. Well known is the lack of Neoproterozoic strata in the entire region from Peru to Central Argentina. In northwestern Argentina, the 'basement' is the Ediacaran to Cambrian Puncoviscana complex (Zimmermann, 2005) and its equivalents. Recently, Bahlburg et al. (2020) identified a low grade meta-sedimentary succession in the Bolivian altiplano, very close to the depositional area of this study, and speculated for a Tonian age. First heavy mineral studies and detrital zircon studies (Reimann et al., 2010; Reimann Zumsprekel et al., 2015) for rocks of this study area show a recycled characteristics with extreme high ZTR values and only a weak reflection of the major orogenic events during the Cambrian and Ordovician in the region. Paleotectonic models (e.g. Ramos, 2000; Chew et al., 2007, 2008; Bahlburg et al., 2009; Rapela et al., 2016) argue for geological processes during the Neoproterozoic which should have produced thick sedimentary successions during the Neoproterozoic. This calls for thick cover sequences of the metamorphic basement which, we think, as a first hypothesis, had been recycled constantly into the adjacent Paleozoic basins. Therefore, we propose as major detrital sources, non-metamorphic (pre-Ordovician to Neoproterozoic aged) sedimentary successions, which are not anymore exposed or may have reworked the detritus (e.g. Iriarte et al., 2021). These sedimentary successions hold the detrital information of the Sunasas belt or Arequipa Massif as identified in the mentioned provenance studies of some of the here studied successions (Bahlburg et al., 2009; Reimann et al., 2010; Reimann Zumsprekel et al., 2015). According to the detrital record here

presented, which has been deposited during the Paleozoic, we understand these successions as compositionally relatively homogeneous and dominated by a felsic composition. The material had not been transported very far and allowed the deposition of a large number of sub-angular to sub-rounded grains. The recycled Ordovician sediments in our study (from Reimann Zumsprekel et al., 2015) may have been developed to quartz-arenites because of the depositional environment, or the source material had been transported longer, and possibly combined with a climate, more destructive to feldspar preservation (e.g. Deng et al., 2022) or/and water composition (e.g. Yuan et al., 2019). Their trace element geochemistry, interestingly, does not differ from the one Paleozoic successions besides slightly evolved Zr/Sc ratios (Figs. 7–10; Tables 1–4). However, more studies on these Ordovician successions is necessary.

4. Conclusions

We developed in northwest Bolivia a geochemical stratigraphy throughout the Paleozoic using nearly 200 geochemical data sets. These data, combined with petrography, does not reveal the expected strong paleotectonic changes reported to the north and south of the study area. In southern Peru and northwest Argentina, Paleozoic sedimentary successions reflect clearly the emergence of an Ordovician and Permo-Carboniferous continental arc (e.g. Bahlburg, 1990; Breitzkreuz and Zeil, 1994; Acenolaza et al., 1996; Zimmermann and Bahlburg, 2003; Bahlburg et al., 2006; Boekhout et al., 2018).

We can only observe Ordovician successions which are highly recycled and texturally as well as compositionally mature (Reimann Zumsprekel et al., 2015) but the trace element composition differs not strongly from all other Paleozoic successions besides slightly higher Zr/Sc ratios. The rocks contain very high Cr and V concentrations which are a detrital signal as tests for all formations in regard of the existence of a major and significant an-oxic depositional environment could not be observed, as well not for the two diamictites, interpreted as glacial deposits (Díaz Martínez and Isaacson, 1994; Díaz Martínez and Grahn, 2007).

We cannot observe any enrichment in non-felsic detritus besides smaller occurrences of pyroclastic material in the Permian Chutani Formation. This, combined with systematic depletion in Nb, Ta and TiO₂ in the same succession may point to the detrital influence of a continental arc, but needs much more substantiation by heavy mineral data in the future.

All post-Ordovician rocks show reworking but there is no trend of an increase in recycling stratigraphically up, wherefore we interpret that any recycling within the stratigraphy was not a major sedimentary process. Instead, extrabasinal sources fed the basin constantly over 200 My with compositionally relatively homogeneous non metamorphic felsic detritus which had been eroded in relatively vicinity. During the late Paleozoic the sediments are less sorted and show a higher variability within the framework components than the older ones within the Paleozoic. This supports earlier basin models, stating a constant decrease of the depositional area and diminishment of the entire Peru-Bolivian trough. The absent of significant metamorphic detritus, besides ultrastable heavy minerals, is astonishing as the basin had been sandwiched between the metamorphic rocks of the Arequipa Massif (to the west) and the Sunasas belt (to the east). It is well known that the stratigraphic record between 900 and 550 Ma in the entire region of the Central Andes is poor or even absent, although thick sedimentary successions should have been deposited, either at an extensional or compressional margin of Westgondwana (according to the favored paleotectonic model). We propose that the northwestern Paleozoic successions in Bolivia consist of this, now eroded, sedimentary package covering the Arequipa Massif and Sunasas belts. These sedimentary cover sequences contained the detrital information of the underlying metamorphic basement, found in provenance studies of Paleozoic rocks within the area (Bahlburg et al., 2009; Reimann et al., 2010; Reimann

Zumsprekel et al., 2015), and detritus was transported only a short distance into the Peru-Bolivian trough.

The absence of significant – ‘typical’ – detritus reflecting the major paleotectonic changes, recorded at the margin of western Gondwana, to the north and south of the study area, implies either (i) very different sediment dispersals compared to the areas to the north and south, (ii) a differing paleogeography towards the west, or (iii) a combination of both. However, this is still speculation, but with this contributions we could set a first orientation for further detailed research in this field.

CRedit authorship contribution statement

Udo Zimmermann: Writing – review & editing, Writing – original draft, Supervision, Resources, Project administration, Methodology, Investigation, Funding acquisition, Conceptualization. **Shirley Lopez:** Supervision, Investigation. **Zohyab Afzal:** Investigation. **Krishiat Alexandra Cuellar Guasde:** Investigation.

Declaration of competing interest

The authors declare that they have no known competing financial interests or personal relationships that could have appeared to influence the work reported in this paper.

Data availability

all data can be used after publication

Acknowledgements

The project had been co-funded by EnPe project ‘Master of Science of Petroleum Geology’ from the Ministry of energy and Petroleum (Norway). We thank the assistance of valuable reviews of two colleagues and are grateful for the kind editorial handling.

Appendix A. Supplementary data

Supplementary data to this article can be found online at <https://doi.org/10.1016/j.jsames.2023.104280>.

References

- Aceñolaza, F.G., Miller, H., Toselli, A., 1996. Geología del Sistema de Famatina. *Munchner Geol. Hefte - Reihe A Allg. Geol.* 19, 1–410.
- Armstrong-Altrin, J.S., Verma, P.S., 2005. Critical evaluation of six tectonic setting discrimination diagrams using geochemical data of Neogene sediments from known tectonic settings. *Sediment. Geol.* 177, 115–129.
- Bahlburg, H., 1990. The Ordovician basin in the Puna of NW Argentina and N Chile: geodynamic evolution from back-arc to foreland basin. *Geotekt. Forsch.* 75, 1–107.
- Bahlburg, H., 1998. The geochemistry and provenance of Ordovician turbidites in the Argentine Puna. In: Pankhurst, R.J., Rapela, C.W. (Eds.), *The Proto-Andean Margin of Gondwana*, vol. 142. Geological Society London Special Publication, pp. 127–142.
- Bahlburg, H., Hervé, F., 1997. Geodynamic evolution and tectonostratigraphic terranes of northern Argentina and northern Chile. *Geol. Soc. Am. Bull.* 109, 869–884.
- Bahlburg, H., Carlotto, V., Cárdenas, J., 2006. Ollantaytambo formation and Umachiri beds: evidence of early to middle Ordovician arc volcanism in the Cordillera Oriental and Altiplano of southern Peru. *J. S. Am. Earth Sci.* 22, 52–65.
- Bahlburg, H., Vervoort, J.D., Du Frane, S.A., Bock, B., Augustsson, C., Reimann, C., 2009. Timing of crust formation and recycling in accretionary orogens: insights learned from the western margin of South America. *Earth Sci. Rev.* 97, 215–241.
- Bahlburg, H., Vervoort, J.D., DuFrane, S.A., Carlotto, V., Reimann, C.R., Cardenas, J., 2011. The U-Pb and Hf isotope evidence of detrital zircons of the Ordovician Ollantaytambo Formation, southern Peru, and the Ordovician provenance and paleogeography of southern Peru and northern Bolivia. *J. S. Am. Earth Sci.* 32, 196–209.
- Bahlburg, H., Zimmermann, U., Matos, R., Berndt, J., Jimenez, N., Gerdes, A., 2020. The missing link of Rodinia break up in western South America: a petrographical, geochemical, and zircon Pb-Hf isotope study of the volcanosedimentary Chilla beds (Altiplano, Bolivia). *Geosphere*. <https://doi.org/10.1130/GES02151.1>.
- Bhatia, M.R., Crook, K.A.W., 1986. Trace elements characteristics of graywackes and tectonic setting discrimination of sedimentary basins. *Contrib. Mineral. Petrol.* 92, 181–193.
- Bock, B., Bahlburg, H., Wörner, G., Zimmermann, U., 2000. Tracing crustal evolution in the southern Central Andes from Late Precambrian to Permian with geochemical and Nd and Pb isotope data. *J. Geol.* 108, 513–535.
- Boekhout, F., Reitsma, M.J., Spikings, R., Rodriguez, R., Ulianov, A., Gerdes, A., Schaltegger, U., 2018. New age constraints on the paleoenvironmental evolution of the late Paleozoic back-arc basin along the western Gondwana margin of southern Peru. *J. S. Am. Earth Sci.* 82, 165–180.
- Breitkreuz, C., Zeil, W., 1994. The late carboniferous to triassic volcanic belt in northern Chile. In: Reutter, K.-J., Scheuber, E., Wigger, P.J. (Eds.), *Tectonics of the Southern Central Andes. Structure and Evolution of an Active Continental Margin*. Springer-Verlag, Heidelberg, pp. 277–292.
- Breitkreuz, C., Bahlburg, H., Delakowitz, B., Pichowiak, S., 1989. Volcanic events in the paleozoic central Andes. *J. S. Am. Earth Sci.* 2, 171–189.
- Calvert, S.E., Pedersen, T.F., 1993. Geochemistry of recent oxic and anoxic marine sediments: implications for the geological record. *Mar. Geol.* 113, 67–88.
- Cardona, A., Cordani, U.G., Ruiz, J., Valencia, V.A., Armstrong, R., Chew, D., Nutman, A., Sanchez, A.W., 2009. U-Pb zircon geochronology and Nd isotopic signatures of the pre-Mesozoic metamorphic basement of the eastern Peruvian Andes: growth and provenance of a Late Neoproterozoic to Carboniferous accretionary orogen on the northwest margin of Gondwana. *J. Geol.* 117, 285–305.
- Cawood, P.A., Hawkesworth, C.J., Dhuime, B., 2012. Detrital zircon record and tectonic setting. *Geology* 40, 875–878.
- Chew, D., Kirkland, C., Schaltegger, U., Goodhue, R., 2007. Neoproterozoic glaciation in the Proto-Andes: tectonic implications and global correlation. *Geology* 35, 1095–1098.
- Chew, D.M., Magna, T., Kirkland, C.L., Mišková, A., Cardona, A., Spikings, R.A., Schaltegger, U., 2008. Detrital zircon fingerprint of the Proto-Andes: evidence for a Neoproterozoic active margin? *Precambrian Res.* 167, 186–200.
- Cordani, U.G., Iriarte, A.R., Sato, K., 2019. Geochronological systematics of the huayna potosí, zongo and taquesi plutons, Cordillera real of Bolivia, by the K/Ar, Rb/Sr and U/Pb methods. *Braz. J. Genet.* 49, e20190016 <https://doi.org/10.1590/2317-4889201920190016>.
- Dalmayrac, B., Lancelot, J.R., Leyreloup, A., 1977. Two-billion-year granulites in the Late Precambrian metamorphic basement along the southern Peruvian coast. *Science* 198, 49–51.
- Deng, K., Yang, S., Guo, Y., 2022. A global temperature control of silicate weathering intensity. *Nat. Commun.* 13, 1781. <https://doi.org/10.1038/s41467-022-29415-0>.
- Díaz Martínez, E., 1995. Evidencia de actividad volcánica en el registro sedimentario del Carbonífero Inferior (Viseano Superior) del Altiplano Norte de Bolivia (16°S), y su relación con el arco magmático de los Andes Centrales. *Rev. Tec. Yacimientos Pet. Fisc. Bolív.* 16, 37–49.
- Díaz Martínez, E., Isaacson, P.I., 1994. Late Devonian Glacially-Influenced Marine Sedimentation in Western Gondwana: the Cumaná Formation, Altiplano, Bolivia, vol. 17. Canadian Society of Petroleum Geologists, Memoir, pp. 511–522.
- Díaz-Martínez, E., Grah, Y., 2007. Early Silurian glaciation along the western margin of Gondwana (Peru, Bolivia and northern Argentina): palaeogeographic and geodynamic setting. *Palaeogeogr. Palaeoclimatol. Palaeoecol.* 245, 62–81.
- Fedo, C.M., Nesbitt, H.W., Young, G.M., 1995. Unravelling the effects of potassium metasomatism in sedimentary rocks and paleosols, with implications for paleoweathering conditions and provenance. *Geology* 23, 921–924.
- Floyd, P.A., Leveridge, B.E., 1987. Tectonic environment of the Devonian Gramscatho basin, South Cornwall: framework mode and geochemical evidence from turbidite sandstones. *Journal Geological Society of London* 144, 531–542.
- Floyd, P.A., Keele, B.E., Leveridge, B.E., Franke, W., Shail, R., Dörr, W., 1990. Provenance and depositional environment of Rhenohercynian synorogenic greywackes from the Giessen Nappe, Germany. *Geol. Rundsch.* 79, 611–626.
- Fortey, R.A., Pankhurst, R.J., Hervé, F., 1992. Devonian trilobites at bull, Chile (42°S). *Rev. Geol. Chile* 19, 133–144.
- Frailick, P., 2003. Geochemistry of clastic sedimentary rocks: ratio techniques. In: Lentz, D.R. (Ed.), *Geochemistry of Sediments and Sedimentary Rocks: Evolutionary Considerations to Mineral-Deposit-Forming Environments*, vol. 4. Geological Association of Canada GEOText, pp. 85–104.
- França, A.B., Milani, E.J., Schneider, R.L., O. López P., J. López M., R. Suárez S., Santa Ana, H., Wiens, F., Ferreiro, O., Rossello, E.A., et al., 1995. Phanerozoic correlation in southern South America. In: Tankard, A.J., Suárez Soruco, R., Welsink, H.J. (Eds.), *Petroleum Basins of South America*, vol. 62. American Association of Petroleum Geologists Memoir, pp. 129–161.
- Hamilton, M.A., Soreghan, G.S., Carvajal, C.P., Isaacson, P.E., Grader, G.W., Di Pasquo, M.M., 2016. A Precise U-Pb Zircon Age from Volcanic Ash in the Pennsylvanian Copacabana Formation, Bolivia, vol. 48. Geological Society of America Abstracts with Programs, p. 6. <https://doi.org/10.1130/abs/2016RM-276278>.
- Hofmann, A., 1988. Chemical differentiation of the Earth: the relationship between mantle, continental crust and oceanic crust. *Earth Planet Sci. Lett.* 90, 297–314.
- Hofmann, A., 1997. Mantle geochemistry: the message from oceanic volcanism. *Nature* 385, 219–229.
- Iannuzzi, R.C., Vieira, E.L., Guerra-Sommer, M., Díaz-Martínez, E., Grader, G.W., 2004. Permian plants from the Chutani Formation (titicaca group, northern altiplano of Bolivia): II. The morphogenus glossopteris. *An Acad. Bras Ciências* 76, 128–138.
- Iriarte, A.R., Cordani, U.G., Basei, M., 2021. Provenance study of phanerozoic rocks from the Cordillera real of Bolivia. *Braz. J. Genet.* 51 <https://doi.org/10.1590/2317-4889202120210036>.
- Jones, B., Manning, D.A., 1994. Comparison of geochemical indices used for the interpretation of palaeoredox conditions in ancient mudstones. *Chem. Geol.* 111, 111–129.

- Lacassie, J.P., Hervé, F., Roser, B., 2006. Sedimentary provenance study of the post-Early Permian to pre-Early Cretaceous metasedimentary Duque de York Complex, Chile. *Revista de la Geología de Chile* 33, 199–219.
- Lehmann, B., Dietrich, A., Heinhorst, J., Métrich, N., Mosbah, M., Palacios, C., Schneider, H.J., Wallianos, A., Webster, J., Winkelmann, L., 2000. Boron in the Bolivian tin belt. *Miner. Deposita* 35, 223–232.
- Litherland, M., Annells, R.N., Appleton, J.D., Berrangé, J.P., Bloomfield, K., Burton, C.C. J., Darbyshire, D.P.F., Fletcher, C.J.N., Hawkins, M.P., Klinck, B.A., Llanos, A., Mitchell, W.I., O'Connor, E.A., Pitfield, P.E.J., Power, G., Webb, B.C., 1986. The geology and mineral resources of the Bolivian Precambrian shield. *British Geological Survey, Overseas Memoirs* 9, 1–153.
- Litherland, M., Annells, R.N., Darbyshire, D.P.F., Fletcher, C.J.N., Hawkins, M.P., Klinck, B.A., Mitchell, W.I., O'Connor, E.A., Pitfield, P.E.J., Power, G., Webb, B.C., 1989. The Proterozoic of eastern Bolivia and its relationship to the Andean mobile belt. *Precambrian Res.* 43, 157–174.
- Loewy, S.L., Connelly, J.N., Dalziel, I.W.D., 2004. An Orphaned Basement Block: the Arequipa-Antofalla Basement of the Central Andean Margin of South America, vol. 116. *Geological Society of America Bulletin*, pp. 171–187.
- McLennan, S.M., Taylor, S.R., McCulloch, M.T., Maynard, J.B., 1990. Geochemical and Nd–Sr isotopic composition of deep-sea turbidites: crustal evolution and plate tectonic associations. *Geochem. Cosmochim. Acta* 54, 2015–2050.
- McLennan, S.M., Hemming, S., McDaniel, D.K., Hanson, G.N., 1993. Geochemical approaches to sedimentation, provenance and tectonics. In: Johnsson, M.J., Basu, A. (Eds.), *Processes Controlling the Composition of Clastic Sediments*, vol. 284. Geological Society of America Special Publication, pp. 21–40.
- McLennan, S.M., Taylor, S.R., Hemming, S.R., 2006. Composition, differentiation, and evolution of continental crust: constraints from sedimentary rocks and heat flow. In: Brown, M., Rushmer, T. (Eds.), *Evolution and Differentiation of the Continental Crust*. Cambridge University Press, pp. 92–134.
- Mégard, F., Dalmayrac, B., Laubacher, G., Marocco, R., Martinez, C., Paredes, J., Tomasi, P., 1971. La chaîne hercynienne du Perou et en Bolivie. *Premiers resultats. Cahiers ORSTOM. Serie Geologique* 3, 5–44.
- Midgley, S.D., Taylor, J.O., Fleitmann, D., Grau-Crespo, R., 2020. Molybdenum and sulfur incorporation as oxanyon substitutional impurities in calcium carbonate minerals: a computational investigation. *Chem. Geol.* 553, 119796.
- Morton, A.C., Hallsworth, C.R., 1999. Processes controlling the composition of heavy mineral assemblages in sandstones. In: Bahlburg, H., Floyd, P.A. (Eds.), *Advanced Techniques in Provenance Analysis of Sedimentary Rocks*, *Sedimentary Geology*, vol. 124, pp. 3–29.
- Naidoo, T., Zimmermann, U., Vervoort, J., 2016. Pre-pampean metasedimentary rocks from the argentinian Puna: evidence for the ediacaran margin of Gondwana or the arequipa-antofalla-western pampeanas block. *Precambrian Res.* 280, 139–146.
- Nesbitt, H.W., Young, Y.M., 1982. Early Proterozoic climates and plate motions inferred from major element chemistry of lutites. *Nature* 299, 715–717.
- Otamendi, J.E., Cristofolini, E.A., Morosini, A., Armas, P., Tibaldi, A.M., Camilletti, J.C., 2020. The geodynamic history of the Famatinian arc, Argentina: a record of exposed geology over the type section (latitudes 27°–33° south). *J. S. Am. Earth Sci.* 100, 102558.
- Pankhurst, R.J., Rapela, C.W., Saavedra, J., Baldo, E., Dahlquist, J., Pascua, L., Fanning, C.M., 1998. The famatinian magmatic arc in the central sierras pampeanas: an early to mid ordovician continental arc on the Gondwana margin. In: Pankhurst, R.J., Rapela, C.W. (Eds.), *The Proto-Andean Margin of Gondwana*, vol. 142. Geological Society of London Special Publication, pp. 181–217.
- Pattan, J.N., Pearce, N.J.G., Mislankar, P.G., 2005. Constraints in using cerium-anomaly of bulk sediments as an indicator of paleobottom water redox environment: a case study from the Central Indian Ocean Basin. *Chem. Geol.* 221, 260–278.
- Ramos, V.A., 2000. The southern central Andes. In: Cordani, U.G., Milani, E.J., Thomaz Filho, A., Campos, D.A. (Eds.), *Tectonic Evolution of South America*. 31st International Geological Congress, Rio de Janeiro, pp. 561–604.
- Rapela, C.W., Verdecchia, S.O., Casquet, C., Pankhurst, R.J., Baldo, E.G., Galindo, C., Murra, J.A., Dahlquist, J.A., Fanning, C.M., 2016. Identifying laurentian and SW Gondwana sources in the neoproterozoic to early paleozoic metasedimentary rocks of the sierras pampeanas: paleogeographic and tectonic implications. *Gondwana Res.* 32, 193–212.
- Reimann, C.R., Bahlburg, H., Kooijman, E., Berndt, J., Gerdes, A., Carlotto, V., López, S., 2010. Geodynamic evolution of the early Paleozoic Western Gondwana margin 14°S–17°S reflected by the detritus of the Devonian and Ordovician basins of southern Peru and northern Bolivia. *Gondwana Res.* 18, 370–384.
- Reimann Zumprekel, C.R., Bahlburg, H., Carlotto, V., Boekhout, F., Berndt, J., López, S., 2015. Multi-method provenance model for Early Paleozoic sedimentary basins of southern Peru and northern Bolivia (13°–18°S). *J. S. Am. Earth Sci.* 64, 94–115.
- Romaniello, S.J., Herrmann, A.D., Anbar, A.D., 2016. Syndepositional diagenetic control of molybdenum isotope variations in carbonate sediments from the Bahamas. *Chem. Geol.* 438, 84–90.
- Segeomin-Ypfb, 2001. Base map. Geological map of Bolivia with background 1, 1000000.
- Shackleton, R.M., Ries, A.C., Coward, M.P., Cobbold, P.R., 1979. Structure, metamorphism and geochronology of the Arequipa Massif of coastal Peru. *J. Geol. Soc.* 136, 195–214.
- Suárez Soruco, R., 2000. Compendio de Geología de Bolivia. *Rev. Tec. Yacimientos Pet. Fisc. Bol.* 18, 1–144.
- Suárez Soruco, R., Díaz Martínez, E., 1996. *Lexico Estratigrafico de Bolivia*. *Rev. Tec. Yacimientos Pet. Fisc. Bol.* 17, 1–226.
- Taylor, S.R., McLennan, S.M., 1985. *The Continental Crust: its Composition and Evolution*. Blackwell Scientific, Oxford, pp. 1–311.
- Vieira, C.E., Iannuzzi, R., Guerra-Sommer, M., Díaz Matrínez, E., Grader, G.W., 2004. Permian plants from the Chutani Formation (titicaca group, northern altiplano of Bolivia): I. Genera pectopteris and asterotheca. *An Acad. Bras Ciências* 76, 117–128.
- Wilde, P., Quinby-Hunt, M.S., Erdtmann, B.-D., 1996. The whole-rock cerium anomaly: a potential indicator of eustatic sea-level changes in shales of the anoxic facies. *Sediment. Geol.* 101, 43–53.
- Winchester, J.A., Floyd, P.A., 1977. Geochemical discrimination of different magma series and their differentiation products using immobile elements. *Chem. Geol.* 20, 325–343.
- Young, G.M., Minter, W.E.L., Theron, J.N., 2000. Geochemistry and palaeogeography of upper Ordovician glaciogenic sedimentary rocks in the Table Mountain Group, South Africa. *Palaeogeogr. Palaeoclimatol. Palaeoecol.* 214, 323–345.
- Yuan, G., Cao, Y., Schulz, H.-M., Hao, F., Gluyas, J., Liu, K., Yang, T., Wang, Y., Xi, K., Lia, F., 2019. A review of feldspar alteration and its geological significance in sedimentary basins: from shallow aquifers to deep hydrocarbon reservoirs. *Earth Sci. Rev.* 191, 114–140.
- Zimmermann, U., 2005. Provenance studies of very low- to low-grade metasedimentary rocks of the Puncoviscana complex, northwest Argentina. In: Vaughan, A.P.M., Leat, P.T., Pankhurst, R.J. (Eds.), *Terrane Processes at the Margins of Gondwana*, vol. 246. Geological Society of London Special Publication, pp. 381–416.
- Zimmermann, U., Bahlburg, H., 2003. Provenance analysis and tectonic setting of Ordovician volcanic sedimentary successions in NW Argentina. *Sedimentology* 50, 1079–1114.
- Zimmermann, U., Niemeyer, H., Meffre, S., 2010. Revealing the continental margin of Gondwana: the Ordovician arc of the Cordón de Lila (northern Chile). *Int. J. Earth Sci.* 99, S39–S56. Supplement 1.
- Zimmermann, U., Lopez, S., di Pasquo, M.M., Andersen, T., Hatløy, S., Mehus, T., Ruud, C., Simonsen, S.L., 2015. Palynology and detrital zircons of the silurian Cancañiri Formation from the Bolivian altiplano. *CIMP, Bergen* 16–19, 09.2015, Conference abstracts.